Strål
säkerhets
myndigheten
Swedish Radiation Safety Authority

Author: Joel Geier

Technical Note

2014:05

Assessment of flows to deposition holes

Main Review Phase

Report number: 2014:05 ISSN: 2000-0456
Available at www.stralsakerhetsmyndigheten.se

SSM perspektiv

Bakgrund

Strålsäkerhetsmyndigheten (SSM) granskar Svensk Kärnbränslehantering AB:s (SKB) ansökningar enligt lagen (1984:3) om kärnteknisk verksamhet om uppförande, innehav och drift av ett slutförvar för använt kärnbränsle och av en inkapslingsanläggning. Som en del i granskningen ger SSM konsulter uppdrag för att inhämta information och göra expertbedömningar i avgränsade frågor. I SSM:s Technical note-serie rapporteras resultaten från dessa konsultuppdrag.

Projektets syfte

Det övergripande syftet med projektet är att ta fram synpunkter på SKB:s säkerhetsanalys SR-Site för den långsiktiga strålsäkerheten hos det planerade slutförvaret i Forsmark. Den specifika målsättningen med detta externa granskningsprojekt är att granska och bedöma SKB:s beräkningar av flödena till deponeringshålen. Fokus ligger på hur SKB har hanterat olika typer av osäkerheter i beräkningarna. Uppskattningen av antalet deponeringshål som det föreligger signifikanta flöden i och fördelningen av dessa flöden har bäring på beräkningen av de tekniska barriärernas integritet och radionuklidflödena från kapslar som har fallerat.

Författarens sammanfattning

SKB: konceptuella modell för flöde genom det sprickiga berget i Forsmark grundar sig i en uppdelning mellan (1) starkt uppspruckna deformationszoner (som beskrivs med en deterministisk geometri) och (2) det glesare sprickiga berget (som beskrivs med en statistisk geometri).

Modellen för de starkt uppspruckna deformationszonerna innefattar flera antaganden som inte är väl underbyggda av data. Detta skulle kunna leda till en underskattning av grundvattenflux genom förvarsvolymen. Påverkan av dessa antaganden bedöms dock vara små i förhållande till osäkerheterna i modellen för det glesa sprickiga berget.

Detta granskningsuppdrag fokuserar framförallt på den statistiska modellen för det glesa spricknätverket i närheten av deponeringstunnlarna i det föreslagna slutförvaret. Denna modell, kallad hydro-DFN modell, beskrivs i form av en statistisk population av skivformade eller rektangulära plan med uniform hydraulisk konduktivitet som representerar sprickor som är slumpmässigt fördelade och riktade i rummet i en given bergvolym. Populationen av dessa plan beskrivs med statistiska fördelningar för geometriska och hydrauliska egenskaper. Vattnet antas flöda enbart genom nätverk som formas slumpmässigt genom skärningar av dessa plattor eller sprickplan.

Hydro-DFN modellen begränsas endast till liten utsträckning av direkta geologiska observationer när det gäller de mest kritiska egenskaperna som kontrollerar nätverkets konnektivitet. Modellen kalibrerades genom trial-and-error justeringar för att förbättra passningen av simulationerna till hydrauliska mätningarna. De parametrar som justerades kontrollerar sprickornas storleks- och transmissivitetsfördelningar. På grund av (i) den

begränsade rumsliga upplösningen och de glesa mätningarna i de djupa kärnborrhålen, (ii) den icke-systematiska kalibreringsansatsen, (iii) en överensstämmelse mellan simuleringarna och observationerna som kan betecknas som svag, samt (iv) en mycket begränsad analys av sensitiviteten till parametervärdena kan den resulterande hydro-DFN modellen inte anses vara en unik beskrivning som ger ett utfall som gränssätter osäkerheterna i bergets hydrauliska egenskaper i förvarsområdet.

SR-Site, och den platsbeskrivande modelleringen som den har baserats på, har endast beaktat mycket få alternativa koncept eller parametriseringar, framförallt när det gäller berget i området kring de föreslagna deponeringstunnlarna. SKB presenterar inga alternativa hydrogeologiska konceptualiseringar av bergvolymen kring det tilltänkta slutförvaret som är oberoende av hydro-DFN modellen. Endast några få alternativa parametriseringar förs vidare för beräkningar av närområdets vattenflux. Dessa alternativ är tre relaterade parametriseringar av korrelationen mellan sprickstorlek och transmissivitet.

Denna gransking har beaktat fyra olika sorters alternativa modeller för den hydrauliska bergdomänen som inte är del av SKB:s analys. Två av dessa beaktar heterogeniteten i sprickintensitet som grundar sig i data från Forsmark, men som inte har uppmärksammats i SKB:s hydro-DFN modell. De andra två beaktar sannolikheten för att flöde är påverkat av kanalbildning i sprickor vars hydrauliska konduktivitet inte är likformig.

Modellerna med heterogen sprickintensitet uppvisade en måttlig ökning (möjligtvis fördubbling) i antalet deponeringshål med relativt höga flöden och upp till en storleksordning större maximala flöden. Dessa modeller kunde också leda till en anhopning av deponeringshål som uppvisar höga flöden i en given realisering av förvaret. De alternativa modellerna med kanalbildning har inte utvecklats tillräckligt för att tillåta kvantitativa förutsägelser av påverkan på flödesfördelningarna. En vidare analys av modeller med stark kanalbildning rekommenderas för att utvärdera dess möjliga effekter.

Projektinformation
Kontaktperson på SSM: Georg Lindgren
Diarienummer ramavtal: SSM2011-3628
Diarienummer avrop: SSM2013-2408
Aktivitetsnummer: 3030012-4053

SSM perspective

Background

The Swedish Radiation Safety Authority (SSM) reviews the Swedish Nuclear Fuel Company's (SKB) applications under the Act on Nuclear Activities (SFS 1984:3) for the construction and operation of a repository for spent nuclear fuel and for an encapsulation facility. As part of the review, SSM commissions consultants to carry out work in order to obtain information and provide expert opinion on specific issues. The results from the consultants' tasks are reported in SSM's Technical Note series.

Objectives of the project

The general objective of the project is to provide review comments on SKB's postclosure safety analysis, SR-Site, for the proposed repository at Forsmark. In particular, the aim of this review project is to review and assess SKB's calculation of flow to deposition holes. The focus is on how SKB has handled different types of uncertainties in the calculations. The estimated number of deposition holes encountering flows and the distribution of these flows has implications on the calculation of the integrity of the technical barriers and radionuclide transport from canisters that have failed.

Summary by the author

SKB's conceptual model for flow through the fractured rock at Forsmark is based on a division between (1) highly fractured deformation zones (described in terms of deterministic geometry), and (2) the more sparsely fractured rock (described in terms of statistical geometry).

The model for the highly fractured deformation zones includes several assumptions that are not strongly supported by data, which may lead to underestimation of groundwater flux through the repository volume. However, the impact of these assumptions on flows to deposition holes is judged to be minor, compared with uncertainties in the model for the more sparsely fractured rock.

This assessment focuses mainly on the statistical model for the sparsely fractured rock in the vicinity of the deposition tunnels in the proposed repository. This model, referred to as the Hydro-DFN model, is described in terms of a statistical population of disc- or square-shaped, uniformly conductive plates, representing fractures, which are randomly located and oriented in a given volume of rock. The population of these plates is described by statistical distributions of geometric and hydraulic properties. Flow is assumed to be entirely through networks formed by chance though intersections among these plates (fractures).

The Hydro-DFN model is only weakly constrained by direct geological observations for the most critical property controlling network connectivity. It was calibrated by trial-and-error adjustments of parameters controlling the size and transmissivity distributions, to improve the match of simulations to hydraulic measurements. Due to the limited resolution and

sparseness of the measurements in deep boreholes, the non-systematic calibration approach, an arguably poor match of simulations to observations, and a very limited analysis of the sensitivity to parameter values, the Hydro-DFN model thus obtained cannot be regarded as a unique description that bounds the uncertainties regarding the hydraulic behavior of the host rock.

SR-Site and the site-descriptive modelling on which it was based have considered very few alternative concepts or parametrizations, particularly for the host rock around the proposed deposition panels. No alternative hydrogeological conceptualizations of the repository host rock are presented that are independent of the Hydro-DFN model. Only a few alternative parametrizations are propagated to the point of calculating near-field fluxes; these are three related parametrizations of the correlation between fracture size and transmissivity.

This review has considered four types of alternative models for the hydraulic rock domain (HRD) that have not been considered in SKB's analysis. Two of these take into account heterogeneity of fracture intensity which was identified based on data from Forsmark, but which has been neglected in the Hydro-DFN. The other two consider the likelihood that flow is channelized within fractures that are not uniformly conductive.

The heterogeneous-intensity models could produce a moderate (possibly twofold) increase in the number of deposition holes with relatively high flows, and up to an order of magnitude increase in the maximum flowrates to be considered. The heterogeneous-intensity models could also produce a clustering of deposition holes that are subject to high flowrates, within a given realization of the repository. The channelized alternative models have not been developed sufficiently for quantitative predictions of the effects on flowrate distributions. Further consideration of strongly channelled models is recommended to evaluate the possible effects.

Project information
Contact person at SSM: Georg Lindgren

Strål
säkerhets
myndigheten
Swedish Radiation Safety Authority

Author: Joel Geier
Clearwater Hardrock Consulting, Corvallis, Oregon, USA

Technical Note 46

2014:05

Assessment of flows to deposition holes

Main Review Phase

Date: December 2013
Report number: 2014:05 **ISSN:** 2000-0456
Available at www.stralsakerhetsmyndigheten.se

This report was commissioned by the Swedish Radiation Safety Authority (SSM). The conclusions and viewpoints presented in the report are those of the author(s) and do not necessarily coincide with those of SSM.

Contents

1. Introduction

This technical note summarizes findings from a review assignment on the topic of flows to deposition holes, which has been conducted as part of SSM's Main Review Phase of the SR-Site safety assessment, covering final disposal of spent nuclear fuel at the Forsmark site.

The SR-Site safety assessment is based on the KBS-3V disposal concept in which waste packages comprising copper-steel canisters, enclosing the spent nuclear fuel, are placed in vertical deposition holes spaced at intervals along a series of tunnels within the proposed repository layout. The canisters are surrounded by a compacted bentonite buffer which, once saturated, is expected to prevent advective transport between the canister and natural groundwater in the fractured rock, so that transport of corrodants, corrosion products, and (in the event that the canister is breached) radionuclides can only occur by the comparatively very slow process of diffusion.

From SSM's Initial Review Phase, issues were identified for further investigation regarding the possibilities for erosion of the buffer (piping erosion or chemical erosion) followed by corrosion of the copper exterior of the canister. The main geosphere variables controlling these processes, other than hydrogeochemistry, mainly concern the distribution of flowrates (or groundwater flux) to and around deposition holes. For chemical erosion of the buffer, these flowrates control how fast colloidal bentonite can be removed to maintain the process. For corrosion after the buffer has eroded sufficiently to expose the copper exterior of the canister, groundwater flowrates control the rates at which corrodants can be transported to the surface of the canister, and corrosion products can be transported away. Finally, in the event that the canister is breached, these flowrates control the rate of mass transfer of dissolved radionuclides, and the initial velocity at which radionuclides move away from the canister until they come into contact with the bedrock and its potential capacity for retarding their transport, by the processes of matrix diffusion and sorption.

This report presents the author's assessment in response to specific questions raised by SSM, together with relevant supporting analysis and technical material, concerning:

1 SKB's conceptual model for flow through the fractured rock at Forsmark and its relevance for representing flow through the fractured rock, particularly considering the role of SKB's Hydro-DFN model;

2 Alternative conceptualizations or hydro-DFN parameterizations that may lead to any significant differences in terms of the number of deposition holes that encounter significant flows and the magnitude of such flows;

3 The derivation of the Hydro-DFN model from the Geo-DFN model.

Factors relating to the sensitivity of SKB's extended full perimeter intersection criteria (EFPC) for the acceptance/rejection of deposition holes are also discussed. This topic will be dealt with more fully in a planned extension of this work, making use of quantitative modelling software.

2. SKB's conceptual model for flow

2.1. SKB's presentation of flow model

SKB's hydrogeological model for Forsmark is developed in terms of three main conceptual divisions of the bedrock, as were defined during the site investigations (Follin et al., 2008; Follin, 2008) and carried forward to the numerical models used in SR-Site (Selroos and Follin, 2010):

4 HSD (Hydraulic Soil Domain) represents the regolith (Quaternary deposits);

5 HCD (Hydraulic Conductor Domains) represents the deterministically modelled deformation zones;

6 HRD (Hydraulic Rock mass Domain) represents the less fractured bedrock in between the deformation zones.

SKB's schematic illustration of this concept is given in Figure 2.1.

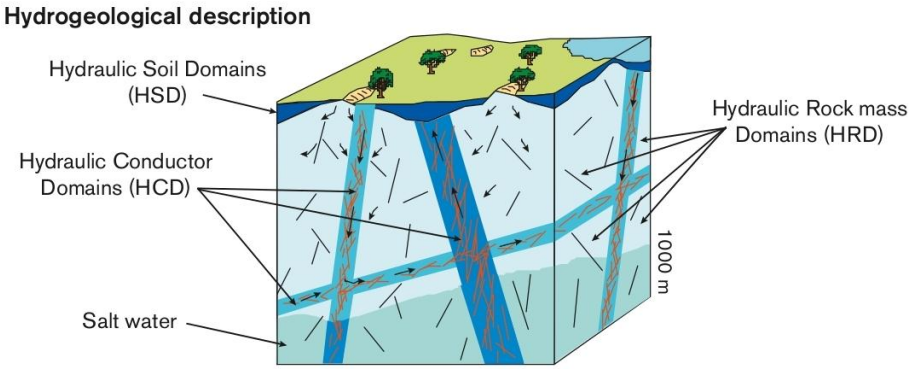

Figure 2.1: Cartoon showing SKB's systems approach used in SDM-Site and SR-Site (from Selroos & Follin, 2010, [SKB R-09-22, p. 33, Figure 3-2])

An additional component not explicitly included in these categories is the shallow bedrock aquifer (Selroos & Follin, 2010, p. 16 and p. 23) which is interpreted as consisting of sheet joints and the gently dipping deformation zones or fractures in the uppermost 150 m of bedrock. In SKB's hydrogeological models this feature has been represented by deterministic, hydraulically conductive horizontal features of finite extent (Follin, 2008, p 76-79).

The HSD pertains to generally shallow Quaternary deposits that lie above the fractured bedrock. This domain will not be given detailed attention in this report, as its influence on flows to deposition holes is minor and can be considered in the context of boundary conditions for flow through the bedrock. SKB's conceptual models for HCDs and HRDs are described in the following paragraphs.

Groundwater flow through this system is driven by the hydraulic gradients that result from local and regional topography, as well as density gradients which are

considered as a function of differences in salinity between brackish Baltic waters and meteoric water that falls on the land surface, and between these waters and waters of higher salinity that are found at depth. According to SKB's site-descriptive model for hydrogeochemistry (Laaksoharju et al., 2008), these more saline waters include relict waters of the Littorina Sea which was roughly twice as saline as the modern Baltic, and deep brines of much higher salinity which are of unknown origin and age.

2.1.1. Hydraulic Conductor Domains (HCDs)

HCDs are considered by SKB to be nominally tabular domains, possibly with curvature on the scale of hectometres to kilometres, but generally with uniform thickness at every point along the defining curviplanar (or piecewise planar) surface. The HCDs are considered to account for all hydraulic conductive features in the modelled domain that are of length scale greater than 1 km.

The hydraulic properties of HCDs are described in terms of transmissivity values which, for a given point on the defining surface, represent the value of hydraulic conductivity integrated across the HCD thickness (e.g., Follin et al., 2008, p. 42).

Transmissivity within a given HCD is described as a negative exponential function of depth (Follin et al., 2008, p. 42; Selroos and Follin, 2010, p. 24):

$$T(z) = T(0)10^{z/k}$$

where z is the elevation (negative of the depth below sea level), k is an empirical constant estimated as 232.5 m (based on a regression fit of the above function to all available measurements from HCDs), and $T(0)$ is an empirical constant deduced from the available measurement(s) for a given HCD. In the case of a single measurement of HCD transmissivity from a borehole that intersects the HCD at a given depth z_i, this constant is calculated simply by inverting the above expression for the given value of $z = z_i$:

$$T = ar^b$$

In the case of multiple measurements $T(z_i)$, $i = 1, \ldots, n$ at various depths in a given HCD, the geometric mean of the $T(0)$ values calculated for each z_i is used:

$$T(0) = \left[T(z_1) \cdot \ldots \cdot T(z_n) \cdot 10^{-(z_1 + \ldots + z_n)/k} \right]^{1/n}$$

In the base model simulation for SR-Site, the only heterogeneity within in a given HCD is due to this function of depth. The transmissivity at a given depth does not vary along strike. SKB refers to this model of HCD transmissivity as the case of "homogeneous HCD" (Selroos and Follin, 2010, p. 59). The resulting zonation of hydraulic conductivity in the HCDs is illustrated in Figure 2.2.

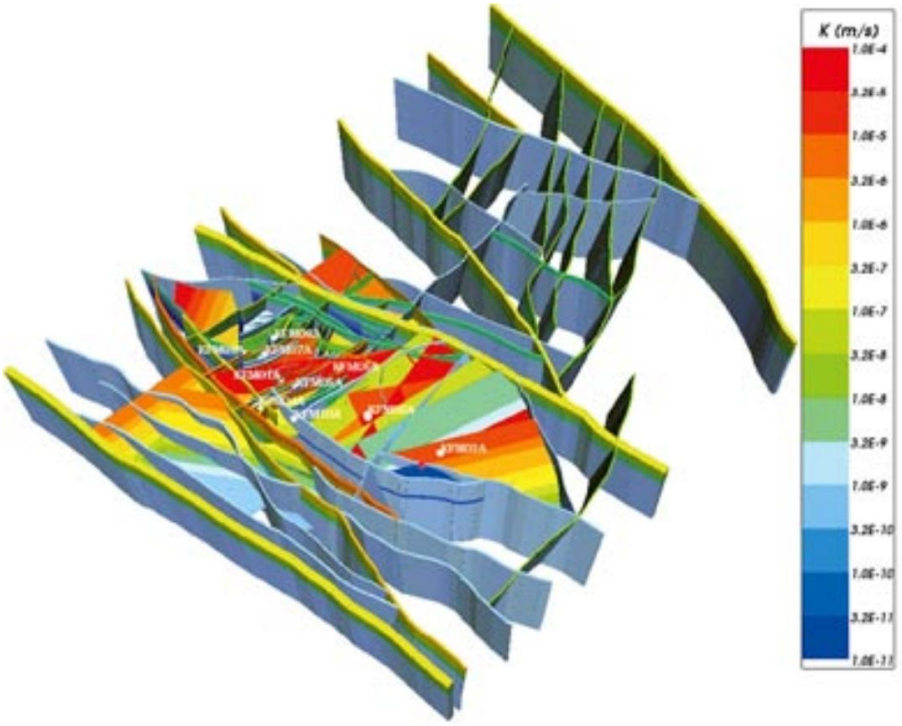

Figure 2.2: HCD model with assigned transmissivities based on depth-trend model, depicted as volumes to show their assigned hydraulic widths. Values of hydraulic conductivity (transmissivity divided by hydraulic width) within each deformation zone are indicated by the colour scale (reproduced from Figure 3-27 of Follin et al., 2008).

Heterogeneity within HCDs along strike is simulated in other ("heterogeneous HCD") calculation cases by adding a random deviate to the exponent of the depth trend:

$$T = T(0)10^{z/k+N(0,\sigma_{\log(T)})}$$

where $N(0,\sigma_{\log(T)})$ signifies the normal distribution with mean value zero and standard deviation $\sigma_{\log(T)} = 0.632$. This value implies a spread of roughly 2.5 orders of magnitude for the 95% confidence interval of $\log(T)$, along strike. In a given realization, a single value of transmissivity is generated stochastically for each triangular patch of the mesh that results from the discretization.

In the heterogeneous HCD cases, values of transmissivity measured in boreholes are assigned to the gridded sections of HCDs that coincide with those points, while random values are assigned elsewhere. HCD transmissivity values are assumed to be uncorrelated between adjacent patches. This approach is equivalent to using a nugget covariance model.

The hydrogeological base case for SR-Site consists of the base model simulation in which the "homogeneous HCD" model (as described above) is used in combination with a stochastic realization of the HRD (as described below), plus 10 stochastic realizations of the "heterogeneous HCD" model, each of which is combined with a separate stochastic realization of the HRD. Selroos and Follin (2010, p. 59) list the following combinations of realizations:

7 Homogeneous HCD + r1 of HRD,

8 r1 of HCD + r1 of HRD,

9 r2 of HCD + r2 of HRD,

…

10 r10 of HCD + r10 of HRD.

where r*n* denotes realisation *n*.

The fact that a single realisation of the HRD (r1) was used in combination both with the "homogeneous HCD" model and one realization of the "stochastic HCD" model allows comparison of these two models of HCD transmissivity variation, in terms of their effects on near-field flows and far-field transport.

In effect, SKB's model of the HCDs amounts to treating each as a tabular aquifer with homogeneous properties across its thickness, and locally isotropic hydraulic conductivity. Heterogeneity is represented as an unstructured random field with uniform patches on the scale of the numerical model discretization.

The HCDs are considered to be deterministically located. A variant is used to test the consequences of additional "possible deformation zones" that were identified in SDM-Site (Selroos and Follin, 2010, p. 76), with heterogeneous transmissivity modelled in the same way as for the "heterogeneous HCD" model described above. Several of these structures intersect the repository tunnels and thus may provide potential flow pathways to or from the deposition zone. According to Selroos and Follin (2010, p. 76), the modelled possible deformation zones have little effect on performance measures (including fluxes to deposition holes).

2.1.2. Hydraulic Rock Domain (HRD)

The HRD in SKB's conceptual model is supposed to account for the hydraulic behaviour of the bedrock, exclusive of the HCDs.

Groundwater flow through the HRD is considered to take place through a network formed by discrete, planar fractures (a discrete-fracture network, or DFN). The DFN model used by SKB for hydrogeological calculations accounting for flow through the HRD is termed the hydrogeological DFN model (Follin, 2008), or Hydro-DFN model for short. The Hydro-DFN model is considered to account for all conductive features in the bedrock of length scale less than 1 km; these features conceptually may include minor deformation zones as well as single fractures.

Each fracture in a stochastic realization of the Hydro-DFN model is considered to have finite extent and to be nominally equidimensional (i.e. a circular disc or a square, depending on the details of numerical implementation).

Each fracture in the Hydro-DFN is characterized by a single value of fracture transmissivity which is considered to be an effective value for network-scale flow, independent of the hydraulic potential gradient and its direction. In applications of the Hydro-DFN model for evaluation of flow in future stages of site evolution, including the early evolution during the construction phase (Svensson and Follin, 2009), temperate phase (Joyce et al., 2009), and future permafrost or glacial stages (Vidstrand et al., 2009), it is also implicitly assumed that fracture transmissivities are not affected by, e.g., changes in rock stresses or precipitation/dissolution processes.

Steady-state flow through the Hydro-DFN is modelled based on the assumption that the 2-D form of Laplace's equation for hydraulic potential holds locally at each point within a given fracture (here the 2-D system of coordinates is within the plane of the fracture), with the constraints of conservation of mass (groundwater flux balance, for incompressible flow) and continuity of the hydraulic potential along the line segment of intersection between any two fractures. The rock between fractures represented in the Hydro-DFN is assumed to be completely impermeable, so groundwater flow is entirely constrained to the connected network of hydraulically conductive fractures.

The fractures are considered to be randomly located within three-dimensional regions called fracture domains, which were established as part of the SKB's geological site-descriptive model development process. This process was guided by interpretations of the bedrock lithology, ductile deformation, and large-scale brittle deformation zones (Stephens et al., 2007), plus statistical evaluation of fracture geometric data from outcrops and borehole mapping. It led to a stochastic description of the fracture population within each of the fracture domains (Fox et al., 2007).

That stochastic description of fracture geometry, termed the "Geo-DFN model" by SKB, is defined in terms of statistical distributions for the following properties of individual fractures belonging to typically five fracture sets (fractures with similar orientations) within a given fracture domain:

11 Fracture size (fracture radius, for disc-shaped fractures);

12 Fracture orientation (fracture pole direction, i.e. unit vector perpendicular to the fracture plane);

In addition, a fracture location model is specified in terms of a stochastic process for the 3-D locations (the centre points) of each fracture.

The Hydro-DFN model for each fracture domain is defined in terms of the statistical distributions for the same properties, plus a statistical model for fracture transmissivity which is defined either as a statistical distribution independent of the other fracture properties, or as a log-linear correlation to fracture size (either perfectly correlated, or with random variations from perfect correlation). Within a given fracture domain, different parameterizations of the statistical model for fracture transmissivity are used for different depth intervals.

As discussed further in Section 3, the stochastic description of fracture geometry in the Hydro-DFN model differs in three key respects from the statistical description in the Geo-DFN model:

13 The fracture size distributions used in the Hydro-DFN model are derived independently, rather than using the fracture size distributions of the Geo-DFN model (although the mathematical form of the distributions used in both the Geo-DFN and the Hydro-DFN are the same, i.e. a power-law distribution, which is also called a Pareto distribution).

14 Whereas the Geo-DFN model development considered a variety of conceptual models for fracture location, only the simplest of these – a uniform 3-D Poisson process characterized by a single parameter, the

volumetric fracture intensity for each fracture set – was considered in the Hydro-DFN model.

15 The volumetric intensity of fractures in the Hydro-DFN is based on the frequency of "open" fractures in core-drilled boreholes (after corrections for directional sampling bias, and adjustments related to the mathematical definition of the power-law distribution for fracture size), while the volumetric intensity of fractures in the Geo-DFN is based on the frequency of all fractures observed on outcrops and in boreholes (after similar corrections); thus the fracture intensity in the Hydro-DFN is assumed to be a subset of the fractures considered in the Geo-DFN.

SKB's conceptual model for groundwater flow through the HRD relies on an assumption that fractures simulated (by the Monte Carlo method) from this statistical description of the "open" fracture population will yield networks of connected fractures that have properties similar to the networks formed by discontinuities in the actual rock, at least in a statistical sense.

Some key characteristics of the final Hydro-DFN model (from Forsmark site descriptive modelling stage 2.2) for the HRD in the vicinity of the repository (fracture domain FFM01 below z = -400 m), forming the basis of SR-Site numerical models for flow in the repository volume, are illustrated by Figure 2.3. The horizontal scale of the simulated region (400 m) was chosen to represent the typical spacing between subvertical HCDs, in this case for simulating flow to a generic vertical borehole.

In SKB's conceptual model, the HCDs effectively act as high-permeability boundaries for blocks of the HRD. It can be seen from Figure 2.3 that although the final Hydro-DFN model contains an abundance of small fractures, the vast majority of these do not belong to networks that connect to the effective hydraulic boundaries. Connectivity on this scale is dominated by a few very large fractures that are on the same scale as the spacing between HCDs.

This outcome is controlled primarily by the probability distribution for fracture size, together with the assumption that flow takes place through uniformly transmissive, disk-shaped fractures. Although different probabilistic models for fracture transmissivity were tested, **the geometrical architecture of the underlying Hydro-DFN model – in effect, the connected pore-space architecture – is the same for all model variants that were used in SR-Site**. The implications of this reliance on a single probabilistic model for the connected pore-space architecture, and the reliability of this model, will be the focus of much of the remainder of this technical note.

Most of SKB's calculations for SR-Site, based on this conceptual model of flow through the HRD, require upscaling from the Hydro-DFN to an equivalent-continuum porous medium (ECPM) representation for at least some portions of the simulation domain. The upscaling is carried out using the CONNECTFLOW code (Jackson et al., 2009, p. 30), by a procedure which involves solving for steady-state flow due to head gradients applied in three orthogonal directions, to each grid block in the HRD representation, and fitting the six independent components of an effective hydraulic conductivity tensor to the fluxes through each face of the block, by least-squares regression.

The calculation of the effective tensor for each block is carried out internally to CONNECTFLOW, and goodness-of-fit measures have not been reported. ECPM tensors were exported from CONNECTFLOW to the DarcyTools code used for simulations of groundwater flows during the initial stages of repository construction, operation, and resaturation (Svensson and Follin, 2009).

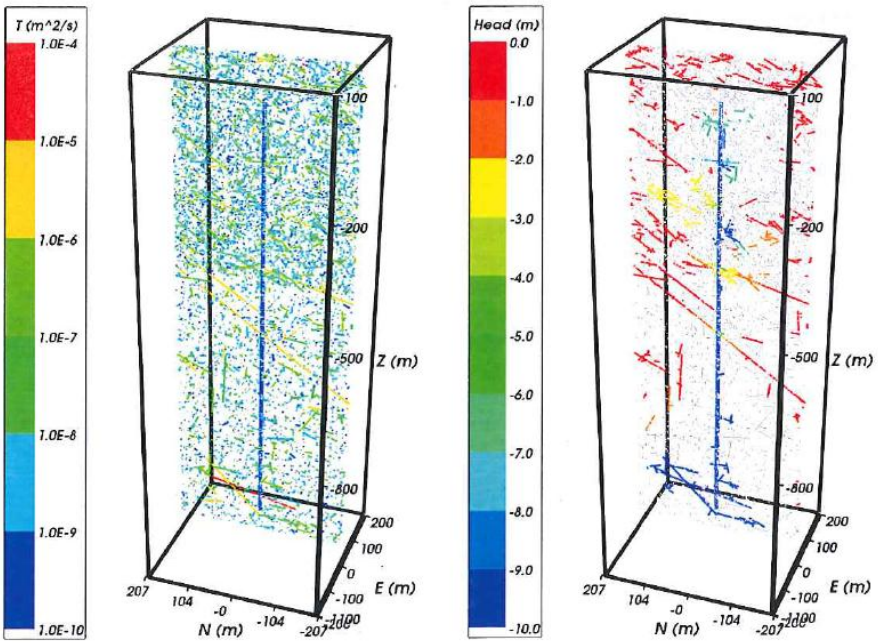

Figure 2.3: (reproduced from Figure 11-14 of Follin et al., 2007a) Vertical cross-section through one realization of the Hydro-DFN for the semi-correlated model of fracture domain FFM01 with different fracture intensity above and below -400 m elevation. Left: all open fractures coloured by transmissivity (a 1 km generic vertical borehole is coloured blue in the middle). Right: all open fractures coloured by drawdown for a simulated pumping test, with unconnected fractures coloured grey.

2.1.3. Complementary information from SKB

SSM requested complementary information on five hydrogeological topics (SSM reference no. SSM2011-2426-109, 2013-03-15). SKB's reply (SKB reference no. 1396324, 2013-05-24) gave responses on four of these topics as described below. SSM's requests and SKB's answers have been freely translated to English to aid the present discussion.

SSM's request: *A discussion of uncertainty in hydrogeological calculations that result from calibration, measurement methods, and the conceptual models. Furthermore it should be explained how these uncertainties are carried forward in the safety analysis in SR-Site with regard to key factor that are meaningful for the results of the analysis (for example distribution of flow to deposition holes, transport distance, and influence of groundwater flow on geochemical stability in the near-field).*

SKB's answer: *This request will be answered in December 2013.*

Reviewer comment: This request is closely related to the subject of this Technical Note, so the observations given herein should be re-evaluated when SKB's response is received.

SSM's request: *SSM requests calculated input data for ECPM simulations for a realization of the so-called base-case hydro-DFN model. More specifically values are requested of hydraulic conductivity, kinematic porosity, and wetted surface per unit rock volume for the ECPM grid cells together with spatial coordinates.*

SKB's answer: *Properties (hydraulic conductivity, kinematic porosity, wetted surface per unit rock volume) for every finite element in the ECPM calculations of the so-called base case of the hydrogeological DFN model have been exported to the Excel file "SSM-properties-question2.xlsx", as attached to this reply. A full explanation of the file contents and of how the information has been taken from the model are in the attached PM (Hartley and Joyce, 2013).*

Reviewer comment: These data have not been used directly in this review. They may be of use for modelling and other calculations to verify SKB's results.

SSM's request: *SSM requests an evaluation of the effective hydraulic conductivity on a 500 m scale for every major rock domain in the northwestern part of the Forsmark site (specifically rock domains RFM029, RFM032 and RFM045). Along with this is requested an account of the points of departure for these evaluations, for example if they are derived from large-scale field measurements, by upscaling from detailed models, or by some other process.*

SKB's answer: *In the attached PM (Hartley and Joyce, 2013) is a detailed description for different evaluations of the hydraulic conductivity in the current rock domains. Evaluations based directly on data as well as evaluations based on DFN modelling are both presented. Furthermore presented are results for different scales (5 m, 20 m, 100 m); however results on the 500 m scale are not presented because this scale is dominated by the effective hydraulic conductivity of deformation zones.*

Reviewer comment: SKB's answer has been examined and is viewed as satisfactory for the needs of this review. The provided data do not factor directly into this review but are useful for general understanding of SKB's results.

SSM's request: *SSM requests a clarification of the measurements and of the hydrogeological assumptions that have been made in the derivation of the correlation between the parameters fracture aperture and fracture flow rate for the Forsmark site. Beyond this is requested a discussion of the consequences of other possible hydrogeological assumptions on the range of these parameter values and evaluation of maximum buffer erosion rates.*

SKB's answer: *In the attached PM (Hartley and Joyce, 2013) is an explanation of how calculated fracture aperture affects buffer erosion, and how previously reported results were used in the calculations. Further there is an account of the consequences of the alternative aperture-transmissivity relationships for buffer erosion.*

Reviewer comment: SSM's request and SKB's answer do not bear directly on this review, as fracture aperture in SKB's models affects advective velocities but not flowrates. However the explanation of relationships for fracture aperture have been

taken into account with regard to SKB's conceptual model for aperture, as part of the Hydro-DFN model.

SSM's request: *SSM requests the calculated distributions of inflow (volumetric flow rate [L3/T] to deposition holes for the so-called base-case in addition to SKB's account of the distributions of equivalent flow and Darcy flux. SSM requests also an account of the equations that are suitable for calculation of inflow to the deposition holes.*

SKB's answer: *The requested data are in the attached Excel file "hydrogeological_base_case_r0_velocity.xls". In the attached PM (Hartley and Joyce, 2013) is given a description of how the values are calculated, specifically which equations are used. As is evident from the answer to this question, the equations are also given in connection with the answer to question number 4 above.*

Reviewer response: These data are primarily useful for comparison with independent modelling, and for direct calculations to verify results of SKB's analyses of erosion rates etc. The data have been briefly examined but have not been used directly in this review.

2.2. Motivation of the assessment of SKB's conceptual model for flow

The foregoing description of SKB's conceptual model for flow through the fractured rock at Forsmark is intended to serve as the basis of an assessment of the relevance of SKB's representation of flow through the fractured rock, particularly with attention to the flowrates to deposition holes. The assessment of relevance is developed mainly in subsequent chapters of this Technical Note.

2.3. The Consultants' assessment of SKB's conceptual model for flow

SKB's conceptual model for flow through the fractured bedrock at repository depth is based on a binary division of the bedrock into a well-connected network of pervasively conductive domains (with length scales ≥ 1 km) which are regarded as deterministic (HCDs), versus the remainder of the rock (HRD) through which flow takes place only via sparsely connected fractures (with length scales ≤ 1 km). This conceptual model has guided SKB's methodology, which has focused on identifying the large-scale structural geological features, investigating their hydraulic properties, and relying on a statistical characterization of smaller-scale bedrock fracturing.

Several assumptions of this conceptual model should be highlighted:

1 Within each HCD, the mean hydraulic conductivity decreases as a negative exponential function with depth.

2 Each HCD is assumed to have locally isotropic hydraulic conductivity and, if heterogeneity is included, this is statistically isotropic (apart from the trend with depth) and uncorrelated over scales larger than the triangular patches that are used to discretize the HCDs.

3 There is no tendency for the locations or properties of fractures in the HRD to depend on their spatially proximity either to other HRD fractures, or to the brittle deformation zones that are represented by the HCDs.

4 Heterogeneity (transmissivity variation or channelling) within features in the HRD, as represented by the Hydro-DFN model, is assumed to be unimportant for large-scale flow and transport, even within the largest features that might represent minor deformation zones on scales close to 1 km.

The first assumption, as pointed out in the initial phase of this review, is only strongly supported by data for the gently dipping HCDs (Figure 2.4). As commented previously (Geier, 2011a):

> *The transmissivity data from deformation zones could just as well support an alternative interpretation in which only the gently dipping zones show a regular pattern of transmissivity decreasing with depth, while the steep zones are essentially random (dominated by heterogeneity which ranges over 5 orders of magnitude) in the interval -100 m to -600 m, then predominantly tight below -600 m. However, such an interpretation, or any other alternative to the assumption of a single trend with depth for all zones, has not been tested for SR-Site.*

The assumption of uniformly decreasing transmissivity with depth can be expected to limit the proportion of groundwater flux that passes through repository depths rather than closer to the surface.

In a memorandum (Hartley et al., SKBdoc id 1416510) giving SKB's responses to an SSM request for complementary information on uncertainties in hydrogeological calculations, further analyses are cited to discuss the relation of deformation zone transmissivity to normal stress. The results are tentative and inconclusive, beyond a statement that the results "***do not falsify*** *the hypothesis that the considerable reduction in the inferred transmissivity data of deterministic deformation zones is* ***partly*** *due to the increasing effective normal stress*" with depth (emphasis added).

The authors of this memorandum note that the lateral heterogeneity within deformation zones is of magnitude comparable to the inferred depth trend. This is not controversial, and indeed, was one motivation for the review comment quoted above. They mention that the variants that included lateral heterogeneity in the deformation zones include patches with elevated transmissivities at depth similar to the mean values at the surface "at some places in each realization," and on this basis they argue that these variants "could be considered a proxy for uncertainties in the depth trend also."

This argument is unconvincing, since even in a model that includes a few isolated high-transmissivity patches in predominantly tight deformation zones at depth, the flows will tend to be dominated by the surrounding, tighter portions of the zones. However, the authors' further argument, that the effects of the HCD model on flows to deposition holes are mitigated by the properties of the DFN model for the HRD, is in line with the conclusions of this review.

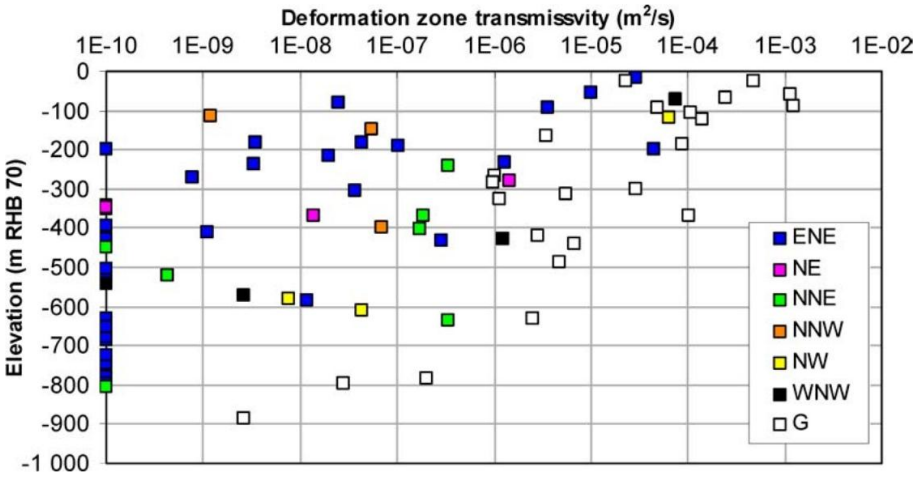

Figure 2.4: Deformation zone transmissivity versus elevation for Forsmark (from SKB R-09-20, Figure 2-4; also in SKB R-09-22 p. 20, Figure 2-6, both based on Figure 5-1 from Follin, 2008). Coloured symbols refer to different sets of deformation zones with different nominal strike directions as listed in the legend; G represents gently dipping zones.

The second assumption, together with the first, precludes the possibility of vertically-oriented bands of elevated transmissivity within a given HCD. Such bands could be expected, for instance, in échelon steps within deformation zones that formed and/or have been reactivated with a strike-slip sense of displacement.

Since transmissivities of adjoining triangular patches (grid cells) comprising a given HCD are assumed to be uncorrelated, the transmissivity fields are unstructured on scales larger than the chosen discretization of the HCDs. SKB has not investigated the consequences of larger-scale correlations such as were modelled by Tsang et al. (1996).

The third assumption – lack of spatial correlation among fractures or their properties – tends to reduce the potential for fractures in a sparse population to form connective networks that are also linked to the HCDs, compared to what would be expected in a fracture population that has a higher degree of spatial structure (e.g. fractal or hierarchical statistical models, or mechanistic models of fracture system development based on structural geological concepts).

The fourth assumption – assumed lack of heterogeneity (such as channelling due to aperture variations) in Hydro-DFN fractures – has been judged by SKB to be of minor importance for far-field radionuclide transport, based on a detailed modelling study by Painter (2006) and subsequent analysis by Crawford (2008). However the potential significance of this assumption for prediction of flowrates to the near field has not been directly assessed. A particular concern, which will be addressed in Section 3 of this technical note, is how the connectivity of the Hydro-DFN model has been affected by a calibration procedure that neglects channelling.

The consequences of these assumptions for flowrates to deposition holes are considered in subsequent sections of this technical note.

SKB's methodology for upscaling from the Hydro-DFN representation to an equivalent continuous porous medium (ECPM) representation is of secondary importance alongside of problems with the underlying detailed model and its calibration. However, gaps in this methodology should also be pointed out. As

noted above, the upscaling is carried out by fitting the components of an effective hydraulic conductivity tensor to the fluxes through each face of the block by least-squares regression (Jackson et al., 2009, p. 30); Joyce and Hartley (2013) also mention an eigenvalue solution which apparently represents a different method for obtaining principal components of the effective hydraulic conductivity tensor.

In either case, the quality of the fits (or numerical stability of the eigenvalue solutions) is not reported. If the fits are poor, this implies a system in which the ECPM upscaling will result in more uniform connectivity than the underlying DFN model, resulting in a less heterogeneous flow system with distributed rather than discrete pathways for transport.

In a sparse network, it is also very possible (even likely) for two adjacent blocks to each be spanned by fractures, but not be connective across both blocks. In such cases, upscaling could potentially lead to exaggerated connectivity in the resulting DFN model. However, this potential issue has been avoided by removing non-connective fractures from the simulations prior to the upscaling calculations. As noted by Follin et al. (2008, p. 68):

> *The isolated fractures are removed based on a regional-scale connectivity analysis, so that ECPM properties are derived only for the network of fractures that contributes to regional-scale flow. If hydraulic conductivity were calculated for an element where connectivity were calculated on the scale of the element, then a higher hydraulic conductivity would probably result, and may be quite scale dependent.*

3. Review of the derivation of the Hydro-DFN model

3.1. SKB's presentation of the derivation of the Hydro-DFN model

The derivation of the Hydro-DFN model for Forsmark stage 2.2, which is used to represent the hydraulic rock domain (HRD) in SR-Site, is documented primarily by Follin et al. (2007a). The main steps in this derivation are summarized in the following subsections.

3.1.1. Data used to derive Hydro-DFN

The Hydro-DFN analysis, as detailed by Follin et al. (2007a), is based almost entirely on data from 21 of the deep core-drilled holes (or 20 such holes, according to Table 6-71 of the SR-Site Data Report, TR 10-52 p. 324) and 32 shallower, percussion-drilled holes, which were available at the time of SKB's data freeze for site-descriptive modelling stage 2.2. The key types of data used are:

- Location and orientation data for fractures identified and classified as sealed, open or partly open from borehole mapping (borehole televiewer logs combined with recovered core samples, which were oriented based on the televiewer logs);
- Constant-pressure hydraulic injection tests in core-drilled holes using a Pipe String System (PSS);
- Differential flowmeter measurements in core-drilled holes under quasi-steady-state open-hole and pumped conditions using the Posiva Flow Log (PFL) tool;
- Impeller flow-logging in combination with pumping in percussion-drilled holes (HTHB method).

The derivation makes limited use of findings from the geological analysis that led to the stage 1.2 Geo-DFN model of La Pointe et al. (2005) or the stage 2.2 Geo-DFN model of Fox et al. (2007), primarily:

- The delineation of fracture domains by Olofsson et al. (2007); and
- The conceptual view of fracture sizes as following a power-law (Pareto) distribution, which was developed within the Geo-DFN analysis based outcrop maps and lineament maps.

Identification of fracture sets is based on "hard sector" ranges of orientation defined by La Pointe et al. (2005).

The actual parameterizations of fracture sets as developed by La Pointe et al. (2005) and Fox et al., (2007) – i.e., the parameters for statistical distributions of fracture orientation, fracture size, and fracture intensity – were not used according to Follin et al. (2007a).

3.1.2. Preliminary analysis of data for Hydro-DFN

A preliminary stage of analysis consists of numerous detailed steps which are listed on p. 121 of Follin et al. (2007a). These can be summarized in terms of the following main steps:

- Classification of fracture data from the borehole mapping according to fracture domains and deformation zones (mainly considering fractures that were mapped in core either as open or partly open; these two categories are lumped together as "open" fractures for the remainder of the analysis);
- Diagnostic plotting and inspection of fracture orientation and fracture intensity data to assess the division into fracture sets and to look for contrasts between fracture domains, between deformation zones and the rock outside deformation zones, and between different depth ranges.
- Diagnostic plotting and inspection of fractures associated with PFL flow anomalies;
- Calculation of fracture intensities (corrected for directional sampling bias) for each of the subdomains of the bedrock that were decided on for the Hydro-DFN representation.

This preliminary stage of analysis leads to various observations which are stated on p. 150 of Follin et al. (2007a). Notable among these are the following (edited for brevity):

- *For both all fractures and open fractures, the HZ set is the most prevalent, followed by the NE set, then the NS and NW set, and the EW set has the lowest intensity;*
- *For PFL fractures, the HZ set is very dominant, followed by the NE.*
- *The intensity of all fractures in deformation zones is on average about 3 times that in the fracture domains, and for PFL fractures, the intensity is five times higher in the deformation zones;*
- *Fracture intensity varies significantly between fracture domains. For open fractures it is highest in FFM02 and FFM04, followed by FFM05. FFM01 has the lowest fracture intensity;*
- *Fracture intensity of open fractures varies strongly with depth. The Terzaghi corrected open fracture intensity averaged over all FFM is about 2 m^{-1} above -200 m, about 1.2 m^{-1} between -200 m and -400 m, and about 0.7 m^{-1} below -400 m. For PFL fractures, the equivalent numbers are about 0.29 m^{-1}, 0.05 m^{-1} and 0.01 m^{-1}, respectively;*

The term “Terzaghi-corrected” refers to a simple geometric correction for directional sampling bias along a line sample (such as a borehole, idealized as by ignoring the finite diameter) that was originally proposed by Terzaghi (1965). The Terzaghi-corrected intensities of open fractures and PFL-associated fractures, mentioned in the last item, are the main quantitative results that are carried forward from this preliminary analysis to the subsequent model development.

3.1.3. Derivation and calibration of the Hydro-DFN model

In the next main stage of analysis, a Hydro-DFN model is derived for each fracture domain by the following sequence of steps (Follin et al., 2007a, p. 164):

1. *Perform DFN simulations of open fractures based on the F 1.2 set and orientation models and based on several different power-law models for fracture size to check the simulated fracture frequency in boreholes for each set.*

2. *Use the open fracture models to perform connectivity analyses to test the simulated frequency of potential flow channels for each of the fracture size models and assess which best reproduce the frequency of PFL flow-anomalies measured in the boreholes.*

3. *Based on step 2, optimise the choice of power-law size parameters for each set to give a frequency of connected fractures consistent with the frequency of PFL flow-anomalies measured in the boreholes.*

4. *Perform DFN flow simulations to calibrate hydraulic parameters and possible relationships between fracture size and transmissivity. The parameters are derived for each set, and potentially with a depth dependency. A direct correlation between fracture size and transmissivity is considered, as well as alternatives based on a semi-correlation and a completely uncorrelated model.*

The first step amounts to a confirmation that the corrections for directional sampling bias have been correctly done, and that fracture orientations and fracture set intensities are adequately characterized by the statistical distributions and correctly simulated by the numerical tools.

The results for Fracture Domain FFM01, as shown in Figure 3.1 (reproduced from Figure 11-7 of Follin et al., 2007a) show good agreement for the sub-horizontal fracture set (HZ) but appear to systematically underestimate estimate the other, subvertical fracture sets (especially the NE- and NS-striking sets), for all five combinations of size-distribution parameters that were tested.

Follin et al. (2007a) suggest introducing an additional subvertical fracture set (striking NNE) to compensate for this systematic error, and give an alternative classification based on this idea on p. 192. However, as stated there, “*This alternative definition of the sets has been derived merely to indicate how much the sets might change using F 2.2 data …. All subsequent modelling in study still uses the F 1.2 sets and orientation distributions*.” Thus this systematic error has been carried forward to the later stages of the Hydro-DFN model derivation.

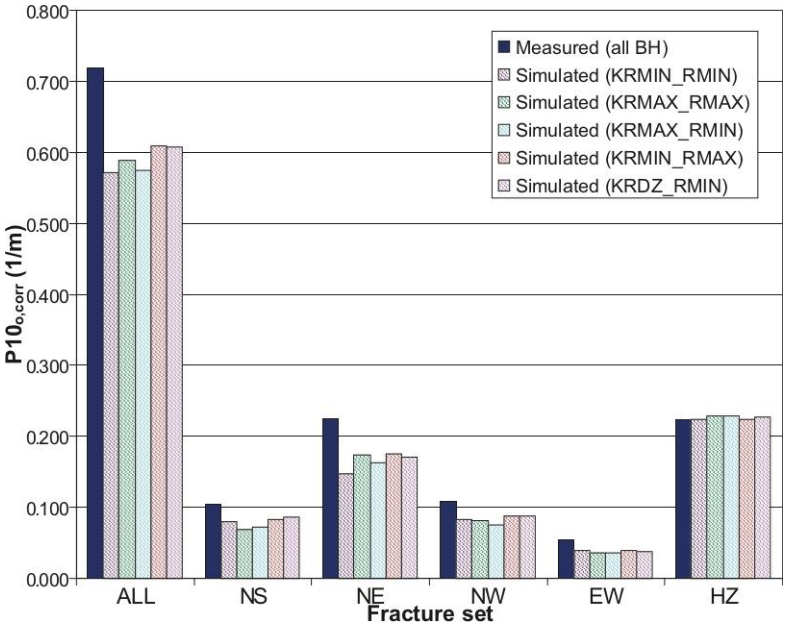

Figure 3.1: (reproduced from Figure 11-7 of Follin et al., 2007a). Comparison of Terzaghi-corrected frequency of open (including partly open) fractures in boreholes $P_{10o,corr}$ as measured, versus simulated values for five different sets of parameters of the fracture size (radius) distribution. ALL = all fracture sets; NS = subvertical set striking N-S; NE = subvertical set striking NE; NW = subvertical set striking NW; EW = subvertical set striking E-W; HZ = subhorizontal set.

The second step, connectivity analyses, is carried out by simulating fractures within a 400 m x 400 m x 1200 m tall domain, for each of the five combinations of size-distribution parameters that were tested. The subset of simulated fractures that are connected via other fractures (or directly) to the boundary of this domain are termed "connected open fractures." This subset is illustrated for two of the trial parameterizations in Figure 3.2.

The frequency of intersections between connected open fractures and a simulated vertical borehole (located in the centre of the domain) after correcting for directional sampling bias, is then obtained as $P_{10,cof,corr}$.

The authors propose that $P_{10,cof,corr}$ should be comparable to the measured frequency (corrected for directional-sampling bias) of PFL anomalies in boreholes, denoted $P_{10,PFL,corr}$ (after correcting in the same way for directional sampling bias based on the orientated of the associated fractures relative to the boreholes). This is based on the idea that fractures only show up as PFL anomalies during sustained pumping, if they are connected via other open fractures to the effective hydraulic boundaries for that volume of rock.

Within SKB's conceptual model, the effective hydraulic boundaries for fractures in the HRD volumes are the HCDs. Follin et al. (2007a, p. 165) state that, "*A 400 m horizontal cross-section was chosen since it is approximately the average spacing between the sub-vertical deformation zones for the local-scale model...*"

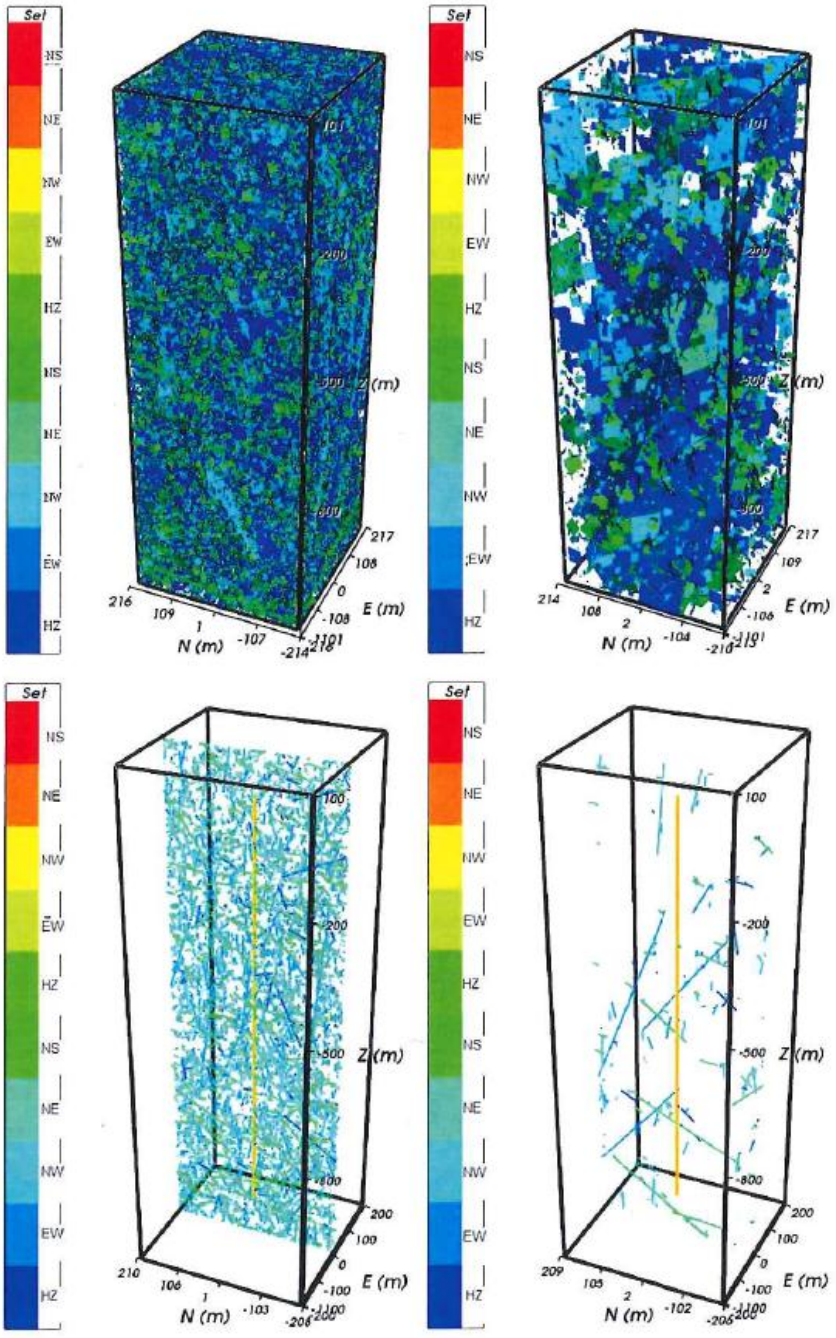

Figure 3.2: (reproduced from Figure 11-9 of Follin et al., 2007a). Visual comparison of connected open fractures for a very well-connected variant (KRKMIN_RMAX) at left, and a more sparsely connected variant (KRKMIN_RMIN) at right, around a single vertical borehole. Top: 3D plots of all connected open fractures. Bottom: a vertical slice through the same networks. Fractures are coloured by fracture sets (5 sets for large fractures $r > 1.1$ m, 5 for small fractures $r_0 < r < 1.1$ m).

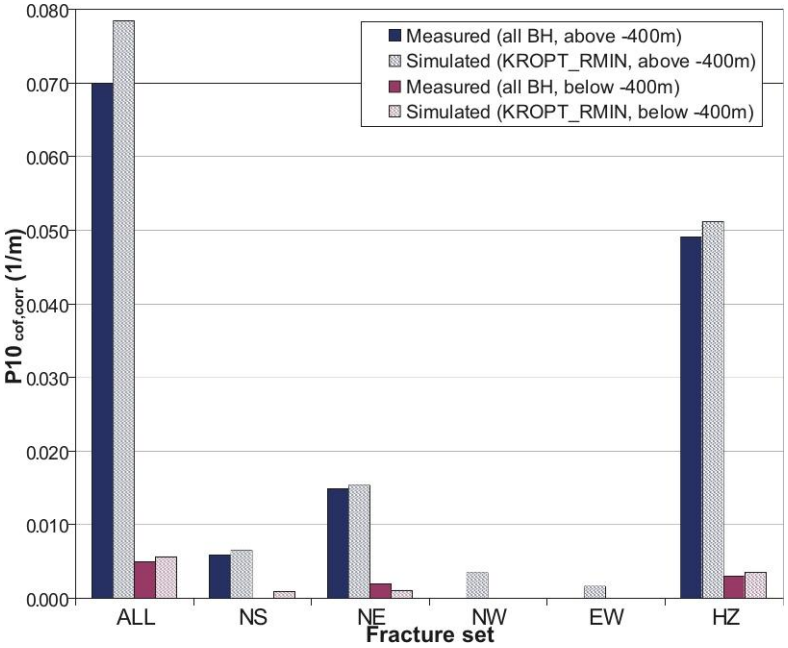

Figure 3.3: (Reproduced from Figure 11-10 of Follin et al., 2007a). Comparison of measured Terzaghi linear intensities of PFL fractures, $P_{10,PFL,corr}$, for fracture domain FFM01 above and below -400 m for each fracture set, versus simulation results of connected open fractures $P_{10,cof,corr}$, for 10 realizations of a vertical borehole for the KROPT_RMIN power-law size model.

As Step 3, after identifying the trial set of parameters for size distribution that gave the best match between $P_{10,cof,corr}$ and $P_{10,PFL,corr}$, out of the five trial parameterizations, Follin et al. (2007a) then adjusted the power-law size parameters for each fracture set and for each depth zone (apparently by a trial-and-error process rather than any more systematic approach such as response-surface methodology) to improve the fit between $P_{10,cof,corr}$ and $P_{10,PFL,corr}$ for all fracture sets in each domain. The results for Fracture Domain FFM01 obtained at the end of this adjustment process are shown in Figure 3.3.

The fourth step aims to derive statistical models for fracture transmissivity (which up until this step has not been considered). Three different types of statistical models are assumed (termed the uncorrelated, semi-correlated, and correlated models) by performing flow simulations in realizations of the DFN model, and adjusting the parameters of three different transmissivity models until a match that is deemed acceptable is obtained.

In mathematical terms, the two "uncorrelated" and "correlated" variants are both special cases of the "semi-correlated" case which is used as part of the reference case:

$$T = 10^{\log\left(ar^b\right)+\sigma N\left(0,1\right)} = ar^b \cdot 10^{\sigma N(0,1)}$$

where $N(0,1)$ is the standard normal distribution, and the units of T and r are assumed to be m^2/s and m, respectively. This may be written more simply and intuitively as:

$$T = ar^b \cdot F(\sigma)$$

where $F(\sigma) = 10^{\sigma N(0,1)}$ is a log-normally distributed "noise factor" with a log mean value of 1. From this form, it is clear that a is the most likely value of transmissivity for a fracture of radius 1 m

If σ = 0 then $F(\sigma) = 1$ (a constant value independent of the realization), so this reduces to the parametric form considered for the correlated variant:

$$T=ar^b$$

while if b = 0 this reduces to the parametric form of the uncorrelated variant:

$$T = a \cdot F(\sigma)$$

Note that SKB uses a different notation for the last case (10^{μ} in place of the factor a). Different values of the parameters a, b, and σ have been used depending on the variant, as listed in Table 3.1.

Table 3.1: Parameters of transmissivity-size model variants for the deep bedrock (z < -400 m) in terms on the general mathematical form $T = ar^b\ 10^{\sigma N(0,1)}$ (based on Table C-1 of Follin, 2008).

Model	a	b	σ
Semi-correlated	5.3×10^{-11}	0.5	1.0
Correlated	1.8×10^{-10}	1.0	–
Uncorrelated	1.6×10^{-9}	–	1.0

The following statistics or measures are mentioned for testing goodness-of-fit (by Follin et al., 2007a, and also on p. 329 of the SR-Site Data Report):

- Average total flow to the abstraction borehole over the 10 realisations.
- Histogram of flow rate to borehole divided by drawdown (notated Q/s) as an average over 10 realisations.
- Bar and whisker plot of minimum, mean minus standard deviation, mean, mean plus standard deviation, maximum of Log10(Q/s) for the inflows within each fracture set taken over all realisations.
- The average numbers of fractures within each set giving inflows to the abstraction borehole above the measurement limit for the PFL-f tests.

Comparisons of simulated vs. field measurements, for the initial, intermediate, and final Hydro-DFN models, are given in tabular form for the first statistic, and in graphical form for the second and third statistics, in Section 11.5 and Appendix B of Follin et al. (2007a). Comparison in terms of the fourth statistic is given numerically in the bar-and-whisker plots. These comparisons are described in the following section.

Figure 3.4 illustrates the differences among the three models by plotting randomly generated pairs of T vs. r based on these different models, and compares these with the approximate measurement threshold for the Posiva flow log in deep core-drilled

holes. It can be seen that the transmissivities assigned by the semi-correlated model imply that most fractures from the scale of the borehole radius up to about 10 m radius are invisible to the PFL measurement method.

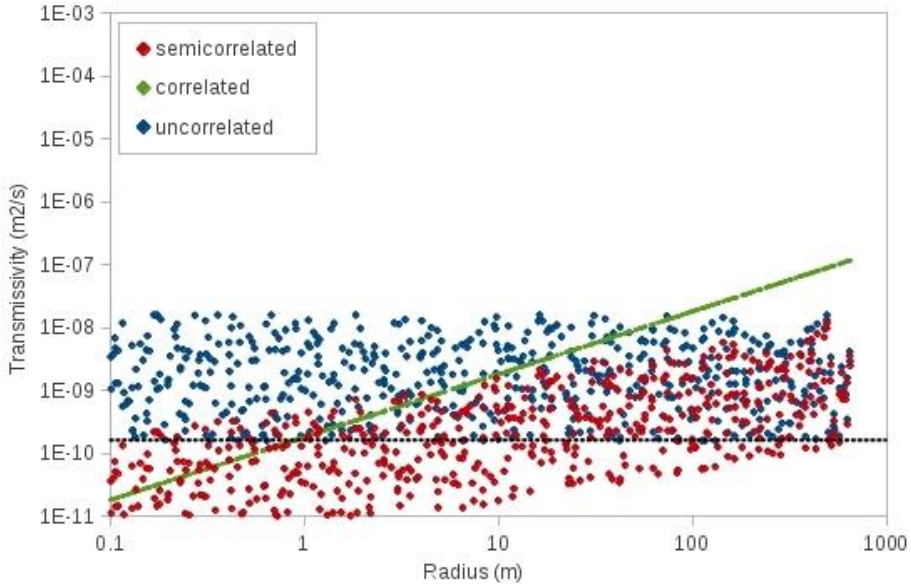

Figure 3.4: Pairs of fracture transmissivity vs. radius generated stochastically based on SKB's semi-correlated, correlated, and uncorrelated model variants for fracture domain FFM01 below *z* = -400 m. The approximate measurement threshold for the Posiva flow log in deep core-drilled holes is plotted as a dashed black line for reference. The number of points is chosen arbitrarily to give a visual impression of the overall trends and spreads of points that can be expected from the mathematical forms of these models.

3.1.4. Simulated vs. field measurements for final Hydro-DFN model of FFM01

The following paragraphs focus on the comparison of simulated vs. field measurements for the Hydro-DFN model of Fracture Domain FFM01. The model for this fracture domain is used for simulations of both FFM01 and FFM06 in SR-Site, and is the most important model for controlling the flowrate distribution to deposition holes.

Average total flow to the abstraction borehole

Comparisons of simulated vs. field measurements of total flow rate divided by drawdown (Q/s) are given in Tables 11-17, 11-19, and 11-21 of Follin et al. (2007a), respectively for the initial Hydro-DFN model of FFM01 prior to adjusting the transmissivity distributions, for a two-layer intermediate model after adjusting the transmissivities, and the final, three-layer model of FFM01.

Oddly the value based on the PFL-f data for measurements below -400 m (representing the near-field host rock for the repository) that this is compared to (total flowrate divided by drawdown, Q/s) changes as a function of the model that is being tested:

- 3.4×10^{-9} m^2/s in Table 11-17 (comparison to the two-layer model before adjusting the T distributions),
- 3.8×10^{-9} m^2/s in Table 11-19 (comparison to the two-layer model after adjusting the T distributions),
- 3.8×10^{-8} m^2/s in Table 11-21 (comparison to the three-layer model after adjusting the T distributions),

It is not clear why this quantity – representing actual data – should change since in all three cases, the data are normalized. Presumably only one of these values is correct.

In any case, the total measured Q/s is lower than what the final (3-layer, semi-correlated) model predicts. If the highest value of 3.8×10^{-8} m^2/s as given in Table 11-21 is correct, then the over-prediction error is only a factor of 1.4, but if one of the other values is the correct one, then the error is more than an order of magnitude (factor of 14 to 16). The highest value appears to be more consistent with the graphical presentation of PFL data in Figures 11-15 and 11-16 of Follin et al. (2007a). The uncorrelated model, in contrast to the semi-correlated model, overpredicts Q/s by a factor of 5.

Histograms of flow rate to borehole divided by drawdown

Histograms of simulated flow rates to boreholes divided by drawdown (Q/s), averaged over 10 realizations of the final, three-layer model for Fracture Domain FFM01, are compared to the corresponding measured quantities in Figure 11-15 of Follin et al. (2007a).

The obtained fits for the final, three-layer model in terms of the second statistic for Fracture Domain FFM01 are shown in Figure 3.5. The main results of interest for this review are those for the portion of FFM01 below -400 m, which represents the near-field host rock for the repository. The differences between the histograms of simulated and measured results, which are readily apparent, are discussed in Section 3.3.

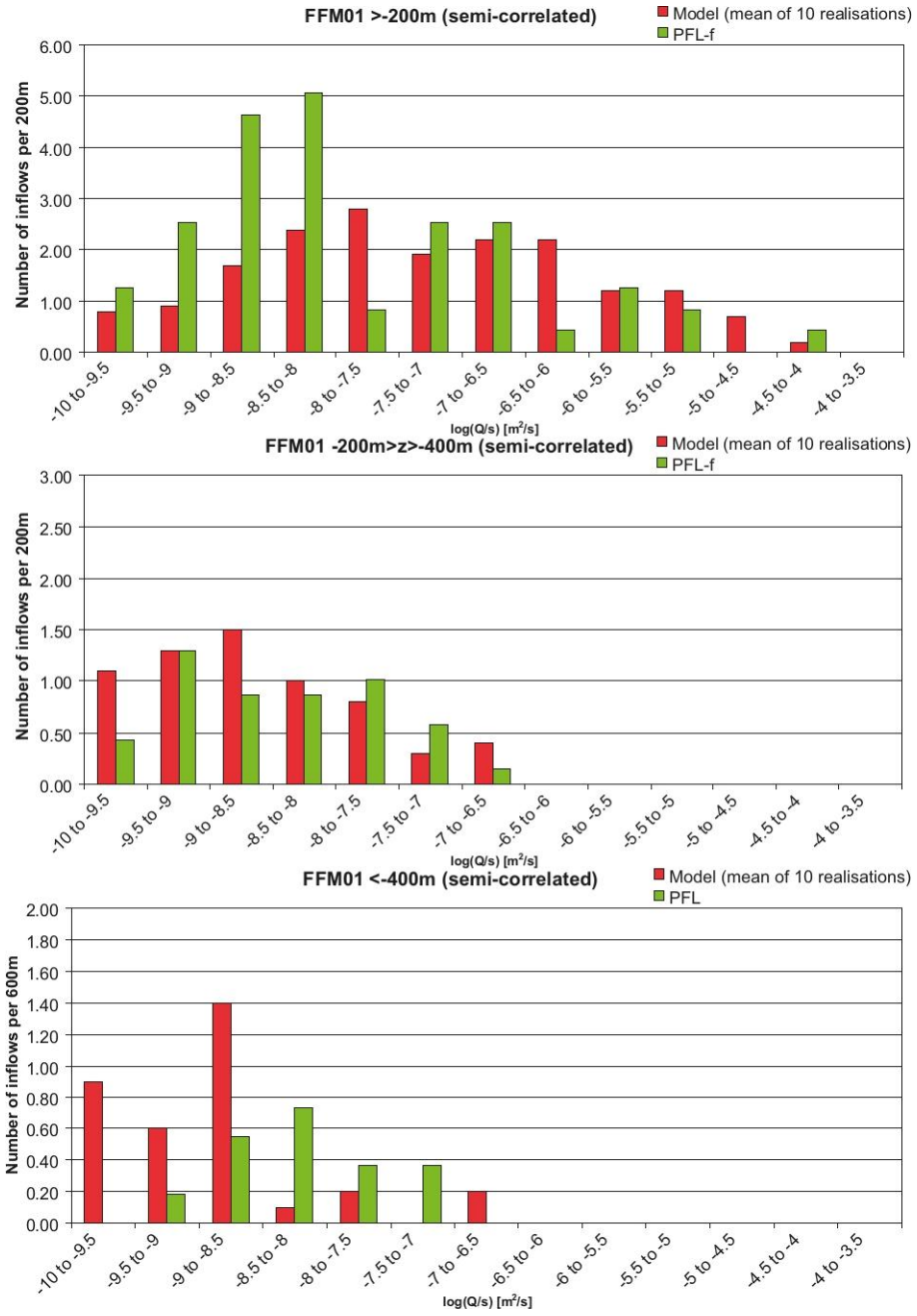

Figure 3.5: (reproduced from Figure 11-15 of Follin et al., 2007a). Histogram comparing the distribution of the magnitude of inflows divided by drawdown, Q/s, at abstraction boreholes in fracture domain FFM01 with a semi-correlated transmissivity (see Table 1120 for parameter values). Top: above an elevation of –200 m; Middle: between –200 m and –400 m; Bottom: below –400 m. The PFL-f measurements are treated as ensemble over all boreholes sections within FFM01. Above –200 m and between –200 m and –400 m, the number of inflows is normalized with respect to a borehole section of 200 m length, and below –400 m relative to a 600 m section. The simulations represent statistics taken from an ensemble over 10 realizations of the Hydro-DFN model.

Statistics of flowrate for different fracture sets

Figure 3.6 reproduces the bar-and-whisker plot presenting statistics for flowrates to different fractures sets, for fracture domain FFM01 below z = -400 m.

From this plot it appears that the model, on average, under-predicts the magnitudes of PFL anomalies associated with both horizontal and subvertical fractures. For subvertical fractures the model assigns inflows to the N-striking set rather than the NE-striking set where they are observed. For the subhorizontal fractures that are associated with most of the PFL anomalies, the model predicts a variance of Q/s similar to the variance of the measurements, but a wider spread of extreme values. Unfortunately the presentation does not indicate how much of this variation is due to differences between stochastic realizations.

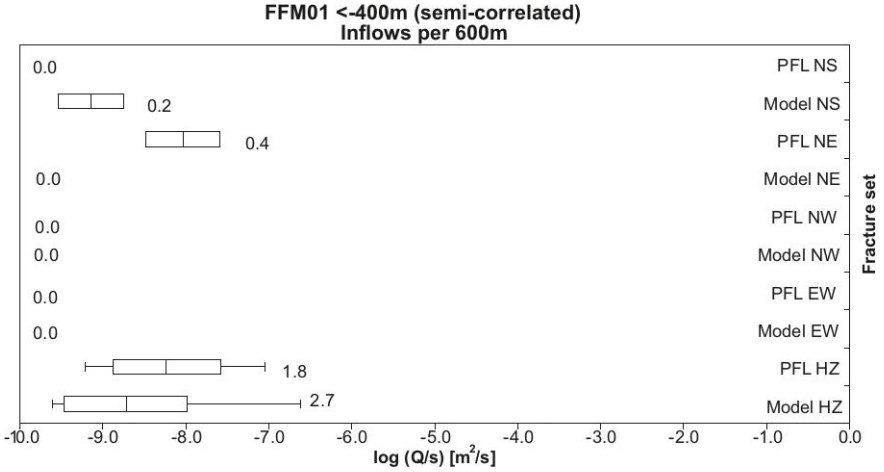

Figure 3.6: (reproduced from the bottom plot of Figure 11-16 of Follin et al., 2007a). Bar and whisker plot comparing statistics taken over each fracture set for the individual inflows, Q/s, for the PFL-f data from borehole sections within FFM01, z < -400 m, against statistics taken from an ensemble over 10 realizations of the Hydro-DFN model with a semi-correlated transmissivity. The number of inflows per inflows per 600 m section of borehole is shown to the right of each bar-and-whisker glyph. For the data, statistics are taken over the fractures generated within each set and an ensemble over 10 realizations.

Average numbers of fractures with PFL measurable inflows

As noted in a previous review by Black (2012), comparisons in terms of this statistic are not discussed in the text after this concept is initially introduced by Follin et al. (2007a). However, the numerical results are shown in the figure reproduced here as Figure 3.6.

A total of 2.2 PFL anomalies per 600 m were measured in the FFM01 domain below -400 m (1.8 anomalies per 600 m associated with HZ fractures, and 0.4 per 600 m associated with NE fractures). This compares with 2.9 simulated anomalies per 600 m in the model (2.7 per 600 m associated with HZ fractures, and 0.2 per 600 m associated with NS fractures).

Thus the calibrated Hydro-DFN model over-predicts the measured frequency of PFL anomalies by 32% (considering all fractures), and by 50% for the subhorizontal fracture set.

3.1.5. Check of geometric consistency between Hydro-DFN and Geo-DFN

A consistency check between the Hydro-DFN model and the Geo-DFN model was furnished in Appendix C of Follin (2008), following a request for this type of comparison by SSM's site-investigations review team (INSITE, 2007, Consolidated Review Issue CRI-22). The comparison for the deep (< -400 m) portion of FFM01, representing the near-field host rock, is shown in Figure 3.7.

The figure indicates that the intensity of open fractures included in the Hydro-DFN model for this domain and depth zone (for a single realization of the model) meets the basic geometrical consistency requirement of being a proper subset of the Geo-DFN model, at least in terms of overall fracture intensity. A check of the consistency in terms of individual fracture sets is not presented by Follin (2008); some convoluted arguments as to why this is difficult are given in the same appendix. A simple check of this requirement is given in Section 3.3.1 of the present review.

This figure also compares the intensity of connected open fractures (*cof*) versus the intensity of open fractures, as a function of fracture radius. This check is not really necessary for demonstrating geometric consistency, as in SKB's methodology the set of connected open fractures is obtained by deleting unconnected fractures from the set of open fractures in a given simulation (so the *cof* fractures are guaranteed to be a proper subset of the Geo-DFN fractures, provided that the open fractures satisfy that requirement).

However, this presentation is informative as to which size ranges of fractures in the Hydro-DFN are likely to be connected to the far-field boundaries. From Figure 3.7 it is clear that, in this DFN model, the vast majority of fractures of radius 10 m or less are not part of a network connected to the boundaries, and thus play no role in conducting flow through the host rock. Even in the size range from about 10 m to 30 m radius, only about 1/10 of the open fractures are connected. On the other hand, nearly all of the fractures of radius larger than about 60 m belong to connected networks, and thus can participate in flow. Thus this Hydro-DFN model for the near-field host rock appears to be dominated by flow through fractures larger than about 60 m.

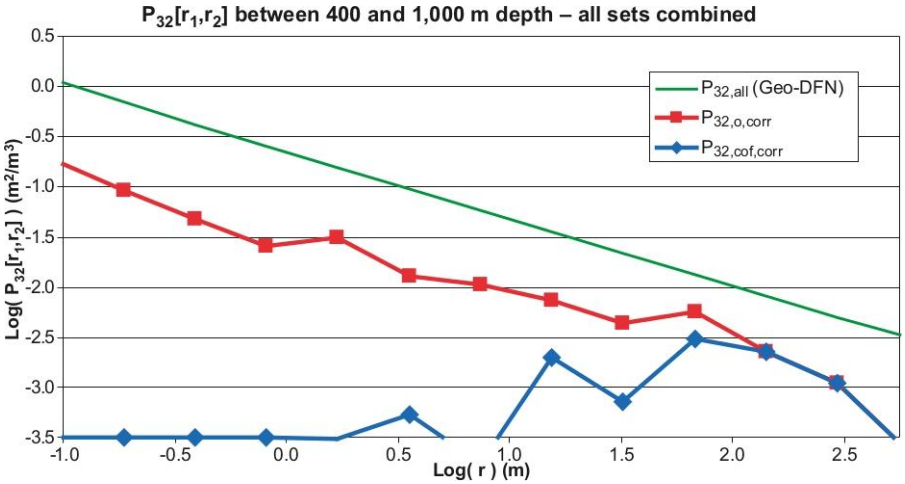

Figure 3.7: (reproduced from Figure C-4 of Follin, 2008). Feature intensity $P_{32}[r_1,r_2]$ as a function of feature size between 400 to 1000 m depth in fracture domain FFM01. The green, red and blue graphs represent the intensity of all features (a), open features (o), and connected open features (*cof*), respectively. The parameters r_1 and r_2 refer to the lower and upper bounds of fracture radius over which the fracture intensity is integrated by the formula in Equation C-3 of the same report. It is not clear from Appendix C-4 of Follin (2008) whether the scale in terms of "Log(*r*)" refers to the lower bound of each interval, r_1, or the upper bound, r_2.

3.1.6. Further adjustments and confirmatory testing

The Hydro-DFN model for the HRD derived by Follin et al. (2007a) underwent several further adjustments as part of the calibration and "confirmatory testing" (comparisons to additional types of field data) of the hydrogeological site-descriptive model for Forsmark, as documented by Follin et al. (2007b).

The calibrations and comparisons included the following main steps as described in Chapter 5 & 6 of Follin et al. (2007b):

- A: Local conditioning on single-hole hydraulic tests. This concerns adjustments to the HCDs rather than the HRD, and is carried out in five substeps.
- B: Matching the 2006 interference test in HFM14 (this focused on reproducing the transient drawdown responses to pumping in HFM14, a percussion-drilled hole that targeted the gently-dipping deformation zone A2 at shallow depth (< 200 m), and mainly resulted in adjustments to the HCDs and HSD, but did lead to an adjustment of vertical hydraulic conductivity in the shallow rock domains above z = -400 m, as explained below).
- C: Matching natural point-water heads: Comparisons were made to heads measured in HFM boreholes (all measurements from the soil or upper bedrock above z = -200 m, and thus do not represent a calibration against heads in the deep bedrock (Follin et al., 2007b, p. 152).
- D: Matching hydrochemistry profiles in boreholes: Comparison is made in terms of salinity, major ions, and pore water composition with results of

modelling the palaeohydrological evolution of the groundwater system during the Holocene (last 10,000 years).

The first three of five substeps in Step A lead to what is referred to as the "stage 2.2 base model simulation," which is used as a central case for further calibration (Follin et al., 2007b, p. 128).

The presentation of the various calibration cases and sensitivity cases explored by Follin et al. (2007b) is very difficult to follow, due to the lack of a systematic, tabular presentation, and a very cumbersome way of referring to the central case and variations on this case. The following acronyms are introduced here in an effort to simplify discussion in this review and make it more precise:

- HCD22 = version of HCD model resulting from substeps 1-3 of Step A
- BMS22 = stage 2.2 base model simulation
- HDFN12 = stage 1.2 Hydro-DFN model derived by Follin et al. (2005)
- HDFN22 = stage 2.2 Hydro-DFN model derived by Follin et al. (2007a)
- K(HDFN12) = ECPM K (hydraulic conductivity tensor) field obtained by direct upscaling of HDFN12
- K(HDFN22) = ECPM K (hydraulic conductivity tensor) field obtained by direct upscaling of HDFN22
- K(HDFN22)vd = modification of K(HDFN22) in which vertical hydraulic conductivities decreased by factor of 10

The calibrations were apparently all performed based on adjustments to a single realization of HCD22, and a single realization of HDFN22.

BMS22 (and thus HCD22) does not include adjustments to hydraulic thicknesses of some HCDs (substep 4 of Step A) or setting minimum values of the HCDs at depth (substep 5 of Step A) to avoid having the deeper portions of HCDs become less conductive than the HRD (Follin et al., 2007b, p. 128):

> *A minimum hydraulic conductivity of 10^{-11} m/s is used within FFM01–06 and 10^{-9} m/s outside the FFM. To avoid this situation, transmissivity divided by thickness is set to a minimum of 10^{-9} m/s for zones described geologically as "regional", and 10^{-11} m/s is used in zones described as either "local" or "local and regional."*

SKB's response to SSM's request for clarification (2012-12-21, Question #17) states that a minimum hydraulic conductivity for the HCD was specified by setting a minimum value for observed transmissivity to 10^{-10} m^2/s where there are no values above the detection limit. This appears to contradict the statement quoted above regarding how the minimum values for HCDs were specified.

Based on statements which appear elsewhere (e.g. on p. 150), BMS22 is based on ECPM22vd rather than ECPM22. Thus apparently:

BMS22 = HCD22 + K(HDFN22)vd + HSD22

where HSD22 refers here to a particular calibrated variant of the HSD model (not discussed further in this review, as the focus is on the deep bedrock).

Of the first three steps A through C, only Step B, matching the interference test in HFM14, provides any measure of the performance of HDFN22 for the repository host rock. The relevance of this test for DFN model confirmation is limited because most of the monitoring intervals at depth are intersected by HCDs which dominate the response, and because of the prior adjustment of HRD properties to produce K(HDFN22)vd, which was done to increase the discrete nature of response in HCDs at depth; specific storage coefficients, properties of individual HCDs, and HSD properties were also adjusted (Follin et al., 2007b, p. 134).

Figure 3.8 shows the measured vs. modelled drawdowns at the end of the interference test, after the adjustments described by Follin et al., 2007b (p. 134), for all of the monitored intervals that included the rock below -400 m. With the exception of the drawdown in KFM04A, the modelled drawdowns after these adjustments described are generally within 1 m of the measured drawdowns. Regarding the residual errors for the intervals in the deeper bedrock, no systematic evaluation of their sensitivity to model parameters has been done, although sensitivities are discussed based on a small set of calculations in which numerous parameters were changed simultaneously.

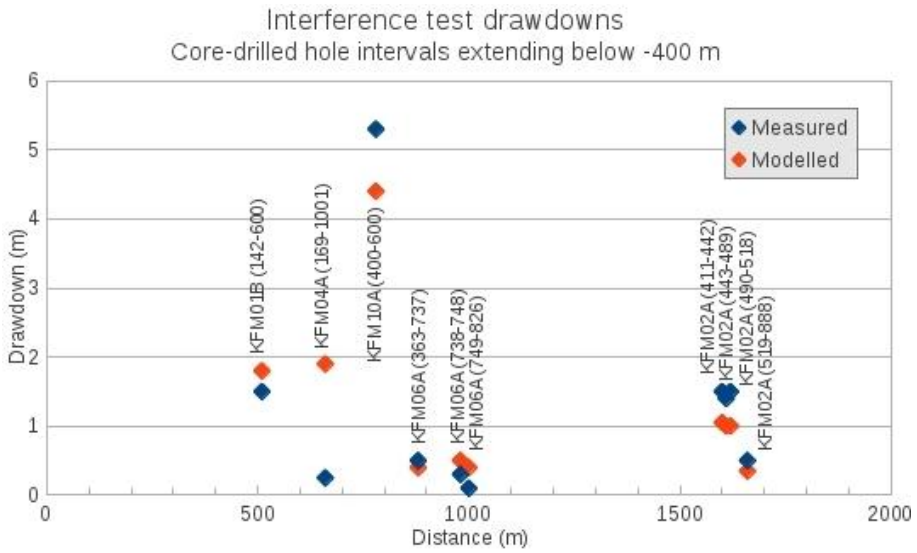

Figure 3.8: (based on values extracted from Figure 5-28 of Follin et al., 2007b). Modelled vs. measured Interference test drawdowns in response to pumping test in HFM14, in monitoring intervals in core-drilled boreholes that include depths greater than 400 m.

Figures 3.9 and 3.10 show more details of the comparison for KFM02A and KFM06A (the deep boreholes that contained the most monitoring intervals for this this test). From the indications of intersections with deformation zones, which are

indicated along the right edge of these plots, it can be seen that all of the monitoring intervals at depths of more than 100 m contained intersections with at least one deformation zone. Thus the observed responses are likely to be dominated by the HCDs rather than the HRD.

Follin et al. (2007b, p. 148) discuss the sensitivities of the HRD to the Step B calibration to HFM14, recognizing that there are large uncertainties in the vertical hydraulic connectivity of the bedrock. They cite incomplete characterization of the fracture sets and orientations and the DFN models based on data from data freeze 2.2, as well as limited core data, borehole imaging logs, and hydraulic measurements in the upper 100 m of rock (due to the telescopic drilling method used for the deep core-drilled holes at Forsmark, which uses percussion drilling followed by casing of the upper section of the hole), as well as directional bias due to mainly vertical boreholes.

The focus of their discussion is on the uppermost part of the bedrock, and leads to several sensitivity cases which are aimed to "*quantify the effects of varying the fracture orientation, and hydraulic conductivity and anisotropy of the upper bedrock.*" These were carried out as variations from the central case BMS22, and include:

- using the older HDFN12 in place of HDFN22;
- using HDFN22 but reducing both horizontal and vertical hydraulic conductivity relative to K(HDFN22) in the upper 400 m of bedrock by one order of magnitude; and
- using HDFN22 but reducing both horizontal and vertical hydraulic conductivity relative to K(HDFN22) in the upper 400 m of bedrock by one order of magnitude.

Both cases give results very similar to those for BMS22. The authors conclude that reductions in hydraulic conductivity by more than one order of magnitude have no further change in the match to the HFM14 hydraulic interference test. However, comparable results are not presented for cases prior to BMS22, i.e. prior to modifying K(HDFM22) to obtain K(HDFM22)vd. This makes it difficult to judge the importance of the reduction of hydraulic conductivity in the uppermost 400 m.

In Step D (matching hydrochemistry profiles in boreholes), according to Follin et al. (2007b, p. 161), the HCD parameterization used was "*based on the calibration steps made for the hydraulic data described*" for Steps A-C (it is not clear if by this they mean the variant termed HCD22 in this review, or the variant that resulted from further modifications of HCD22 in substeps 4 and 5 of Step A).

The HRD parameterization is stated to have been modified:

> *"to reduce the vertical hydraulic conductivity of the HRD either by [1] using the alternative fracture orientation distributions recommended by /Follin et al. 2007b/, as also found in the hydraulic calibration steps described in Section 5.2.2, or [2] by reducing the vertical hydraulic conductivity by one or two orders of magnitude*,"

The "alternative fracture orientations" referred to are in the first case [1] are those used in HDFN22, so this seems to indicate K(HDFN22) rather than K(HDFN22)vd. The second case [2] apparently means a 1-2 order of magnitude reduction of vertical K relative to K(HDFM12), so this is not the same as K(HDFM22)vd.

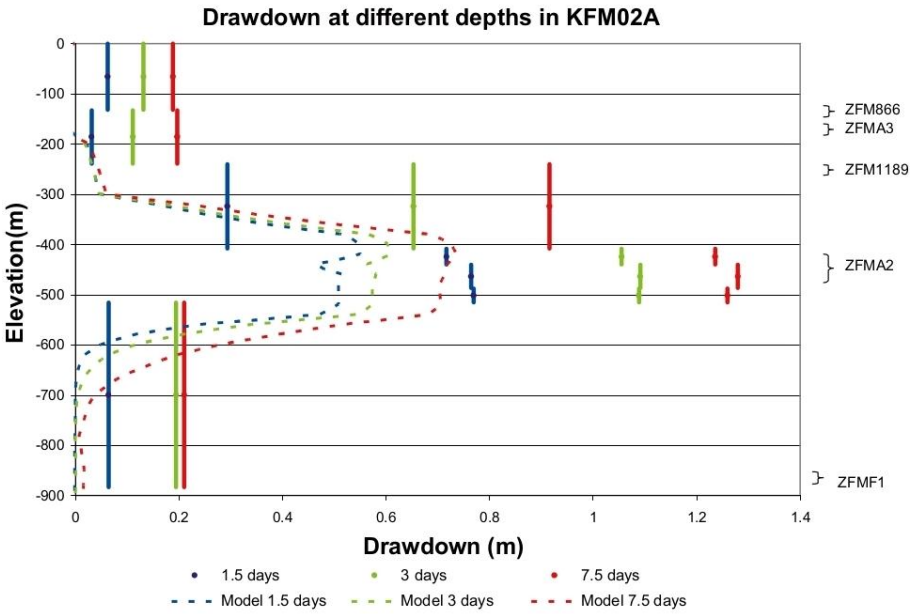

Figure 3.9: (reproduced from Follin et al. 2007b, Figure 5- 11). Comparison of measured (solid) and BMS22 (dashed) drawdown at 3 times for the KFM02A monitoring hole. For the data, a vertical line shows the extent of the monitoring section with the drawdown representing an average within the interval, while the simulated spatial variation in drawdown in the borehole is shown for the model.

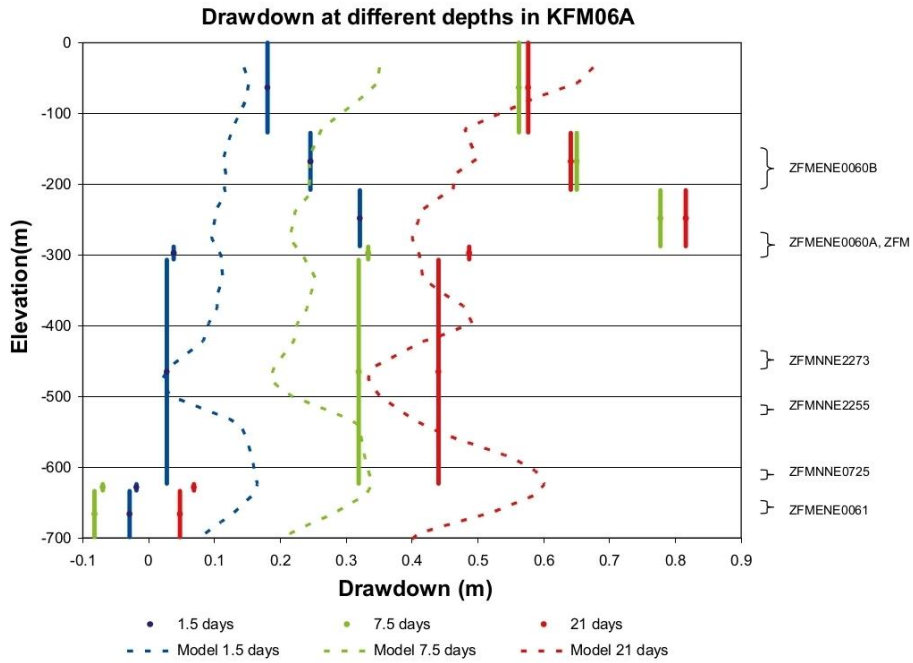

Figure 3.10: (reproduced from Follin et al. 2007b, Figure 5- 12). Comparison of measured (solid) and BMS22 (dashed) drawdown at 3 times for the KFM06A monitoring hole. For the data, a vertical line shows the extent of the monitoring section with the drawdown representing an average within the interval, while the simulated spatial variation in drawdown in the borehole is shown for the model.

Additional modifications are made to parameters affecting solute transport:

- to increase the kinematic porosity by a factor of about 5–10, and
- to use low values of the flow wetted fracture surface area per unit volume of rock (a_r < 0.2–0.3 m^2/m^3)

in order to reproduce the interpreted non-equilibrium between the hydrochemistry in the fractures and matrix over thousands of years. The a_r values are noted to be consistent with PFL flow anomaly data, but the authors do not compare these to estimates that result directly from the Hydro-DFN model. Different values of a_r are used in the paleohydrogeological simulations for SR-Site (SKB R-09-20 Appendix C, Table C-2, p. 144).

Follin et al. (2007b) give comparisons of model predictions with hydrogeochemical measurements for a "*reference calibration case*" which they state is the same as the "*central calibration case used in the hydraulic interference test modelling*" (apparently BMS22, but this is another example where the presentation is ambiguous). If this is the same as BMS22, then it does not seem to line up exactly with the Step D calibration procedure listed above. This question was raised by SSM in a request for complementary information. SKB's reply (2012-12-21, Question #23) acknowledges that "the nomenclature is unfortunate in places" and states that these cases are "essentially" the same, but with extra settings introduced for each type of calibration in terms of boundary conditions and initial conditions.

Results for this "*reference calibration case*" are given as Figures 6-1 through 6-9 of Follin et al. (2007b). The authors interpret the agreement for salinity (reproduced here as Figure 3.11) as "*generally good with significant salinity encountered from about –100 m [below the reference surface datum] associated with Baltic/Littorina Sea Water concentration and then gradually rising below about –500 m [below datum]*." They note some discrepancies with "supplementary" data for KFM07A and KFM09A, and suggest that these might be explained by "*localised heterogeneity or upconing by the intrusion of the borehole."*

However, considering just the deep bedrock below -400 m, large discrepancies can also be noted with more "representative" data from KFM03A, as well as "supplementary" data from KFM02A and KFM08A, and a less severe discrepancy with one more "representative" sample from KFM08A. Considering that the dataset contains only 7 samples that are judged to be at least "somewhat representative," and considering the many adjustments, it is arguable whether these data can be considered as confirmatory of the stage 2.2 Hydro-DFN model. Inspection of the plots for other hydrogeochemical data leads to similarly ambiguous conclusions.

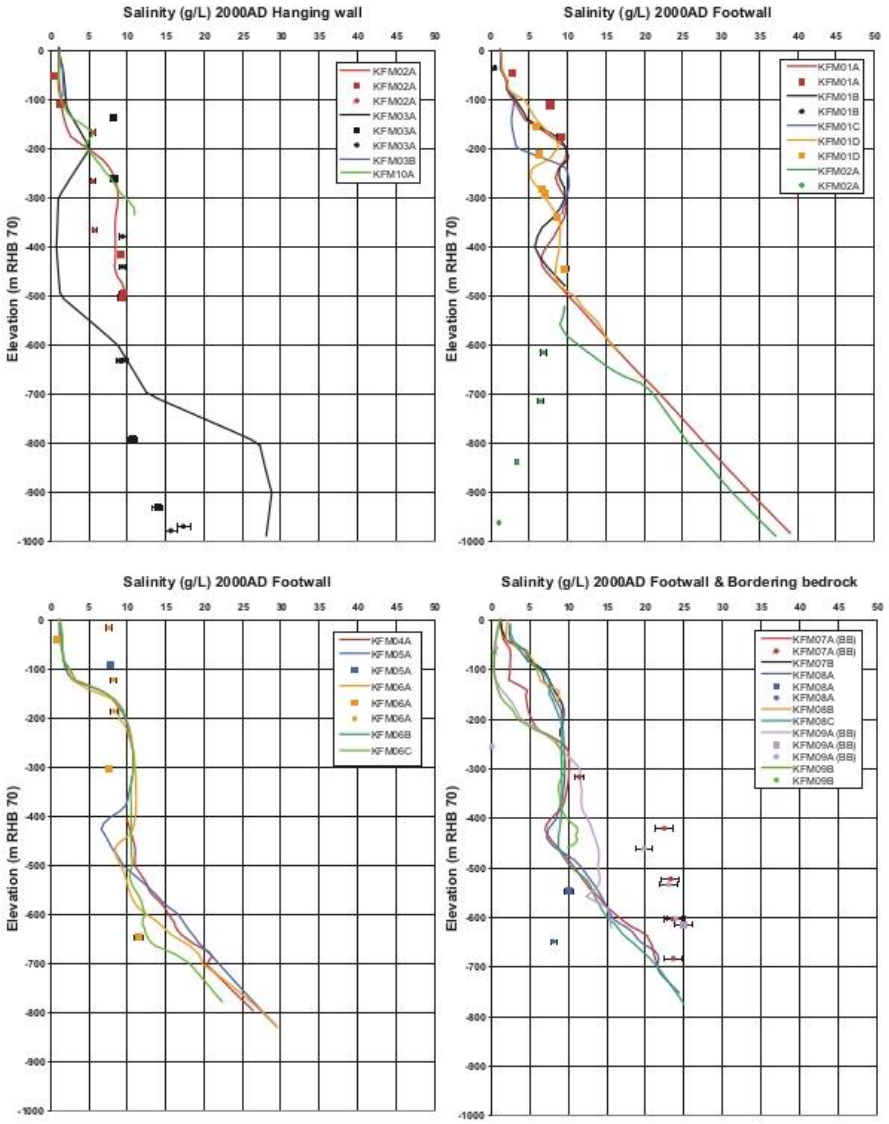

Figure 3.11: (reproduced from Figure 6-1 of Follin et al., 2007b). Comparison of modelled and measured distribution of salinity (TDS) in the fracture system for different groups of calibration boreholes. Square symbols indicate the data which have been classified as “representative” or “less representative.” Small filled circles indicate “supplementary” data which are considered to have relatively high uncertainties. The error bars on the data only indicate the laboratory analytical error, not other sources of error. The solid lines show the simulated distributions in the fracture system. The data in KFM04A above –400 m RHB 70, in KFM07A below –650 RHB 70 and in KFM0 9A below –250 m RHB 70 represent conditions in the bedrock bordering the tectonic lens.

Sensitivities to properties of the Hydro-DFN parameters are investigated only by cases which compare the fracture sets used in HDFN12 or modifications of K(HDFN12).

Further development of SKB's hydrogeological model for Forsmark (Stage 2.3) is presented by Follin et al. (2008). Following the introductory sections, 58 pages (p. 17 through p. 74) are devoted to a recapitulation of the stage 2.2 model

development, which has been discussed above. Changes in stage 2.3 from the stage 2.2 model are described in Section 5.2. The main changes concern more detailed representations of heterogeneity and anisotropy in the HSD. An improved algorithm for simulating heterogeneity in the HCDs while matching local measurements of HCD transmissivity is also introduced, but has only minor effects on the previous model.

The next section of Follin et al. (2008), titled "Calibration of the stage 2.3 base model simulation," gives no details on calibration procedures but presents plots showing comparisons of modelled results vs. measurements, for the same set of calculation cases considered in Steps A-D of the stage 2.2 model calibration. The outcomes in terms of observations in the deep ($z < -400$ m) portion of the site are generally similar to those obtained with BMS22; Follin et al. (2008) note "much better agreement" for point-water heads in the near-surface, and "slight" improvements in terms of hydrogeochemistry. However the only examples of improvements mentioned on p. 87 pertain to the shallow bedrock.

A more organized set of sensitivity cases than seen in previous modelling stages is presented in Section 7.5 and Table 7-2 of Follin et al. (2008). Ten of the "sensitivity cases" are combinations of the HCD model with 10 different realizations of the HRD (Hydro-DFN model). No parametric variations in the HRD model are considered.

The last major report describing the hydrogeological site descriptive model development for Forsmark (Follin, 2008), is a summary of the preceding reports. No significant new information is presented regarding the Hydro-DFN model for the rock below $z = -400$ m, except for a comparison of the Hydro-DFN to the Geo-DFN in Appendix C, which is discussed further in Section 3.3.1 of this review.

3.2. Motivation of the assessment of the Hydro-DFN derivation

The Hydro-DFN model, particularly in its representation of the repository host rock (fracture domains FFM01 and FFM06 at depths greater than 400 m), plays a central role in SKB's predictions of flow to deposition holes. An assessment of the assumptions and data support that are used in the derivation, and of the uniqueness of the resulting model as a description of the bedrock hydrogeology, is important for judging the reliability of this model and the conclusions that it is used to support.

3.3. The Consultant's assessment of the Hydro-DFN model derivation

3.3.1. Relationship of Hydro-DFN and Geo-DFN models

The relationship of the Hydro-DFN to the Geo-DFN models developed for Forsmark SDM stage 1.2 by La Pointe et al. (2005) and for Forsmark SDM stage 2.2 by Fox et al. (2007) has been a source of confusion, due in part to a lack of a clear explanation of the relationship between these models in SKB's top-level documentation, and misleading statements in the discussion which seem to imply that the Hydro-DFN was derived as a subset of a Geo-DFN model (for example Follin, 2008, p. 25-26 and particularly Figure 2-4; also the caption of Figure 11-2, Follin et al., 2007a).

A key point to understand is that the Hydro-DFN model for Forsmark stage 2.2 is not derived directly from either of these Geo-DFN models. Thus it makes minimal use of the structural geological and statistical analysis that contributed to those models. The clearest statement of this is given by Follin et al. (2007a):

> *"The global Geo-DFN model derived for Forsmark stage 1.2 was used as a starting point. However, it is noted that the only significant result of that work used here is the hard sector classification of the fracture sets based on orientation."*

This statement is slightly too categorical, as the Hydro-DFN adopts several other results of the Geo-DFN analysis, mainly:

- the delineation of fracture domains by Olofsson et al. (2007); and
- the conceptual view of fracture sizes as following a power-law (Pareto) distribution, which was developed within the Geo-DFN analysis based outcrop maps and lineament maps.

However in most other respects, the Hydro-DFN represents a completely separate line of analysis.

Whereas the Geo-DFN model of Fox et al. (2007) includes a sophisticated examination of spatial heterogeneity in the fracture population within a given fracture domain – examining, for example, possible correlations between fracture intensity and large-scale deformation zones, possible fractal structure within the fracture population, and spatially variable fracture intensity characterized by a gamma distribution – the Hydro-DFN model development has considered only the simplest type of model, a 3-D Poisson process with a uniform expected value for fracture intensity throughout each domain.

The Hydro-DFN also has not made direct use of the fracture size distributions that were inferred in the Geo-DFN analysis from the best available exposures (surface outcrops) in combination with borehole data. The mathematical form of the fracture size distribution (power-law) has been adopted, but the derived size parameters were not carried over to the Hydro-DFN model.

The lack of direct coupling between the Geo-DFN and the Hydro-DFN means that the parameters of the Hydro-DFN – in particular the parameters controlling the size distribution – are effectively unconstrained by the Geo-DFN model that was developed from surface as well as subsurface structural geological data. Indeed, as acknowledged in Appendix C of Follin (2008), the differences are so great that a direct comparison to check consistency becomes difficult.

The consistency check between the fracture size distributions in the Hydro-DFN and Geo-DFN models, as given in Appendix C of Follin (2008), followed a request for this type of comparison by SSM's site-investigations review team (INSITE, 2008, Consolidated Review Issue CRI-22):

> *"[I]n the Site Descriptive Models 2.2, INSITE notes a divergence of models for the geometry of smaller-scale features which are treated stochastically (discrete-fracture networks, or DFNs), especially between geology (Geo-DFNs) and hydrogeology (Hydro-DFNs).*

"Where previous versions of the Hydro-DFNs were derived from the Geo-DFNs, ensuring geometric consistency, the current Hydro-DFNs have loosened the reliance by calibrating size-distribution parameters directly to flow anomalies observed with the Posiva Flow Log (PFL). INSITE considers that the relationship of Hydro-DFN geometric parameters to PFL anomalies is poorly constrained. Alternative conceptual models, for instance channelised fractures, could give rise to Hydro-DFN models that match the data equally well, but have very different implications for geochemical stability of the near-field and radionuclide transport in the far-field.

"INSITE understands SKB's contention.... that there are likely enough fractures in the Geo-DFNs to account for the Hydro-DFNs as subsets. However, this should be demonstrated quantitatively. Just as importantly, the relationship between the Hydro-DFNs and Geo-DFNs should be explained. In past versions of the SDMs, this relationship was explained in terms of correlation models that offered some possibility for quantitative testing.

"... Therefore INSITE expects that SKB should (1) demonstrate geometrical consistency of the new Geo- and Hydro-DFNs, and (2) present explanations for the relationship between the two types of models, framed as hypotheses that can be tested and confirmed (or adjusted) in underground investigations."

The second paragraph of this comment relates to SKB's implicit assumption, in the Hydro-DFN derivation, that flow takes place uniformly through nominally disk-shaped fractures (represented as squares in CONNECTFLOW) rather than through elongated channels; this issue and its implications will be discussed in detail in Section 3.3.3 of this assessment.

The third paragraph was addressed in part by Appendix C of Follin (2008), including the plot that is reproduced as Figure 3.7 of this technical note. This plot, based on a single realization of the Hydro-DFN model, addresses the question of geometric consistency by comparing the total fracture intensity of fractures (as a function of radius) in the Geo-DFN model, versus the total intensity of open fractures in the Hydro-DFN realization for FFM01 below -400 m.

The use of a single stochastic realization leads to some uncertainty, particularly with regard to open fractures larger than 100 m which (in Figure 3.7) appear to exceed the total fracture intensity for the same sizes of fractures, in the Geo-DFN. This is possibly an artefact of the stochastic simulation in a finite generation region, which can lead to excessive generation of large fractures when using a power-law distribution.

A comparison independent of these stochastic simulation artefacts is possible by considering the integral of fracture area over finite intervals of fracture radius:

$$\int_{r_1}^{r_2} f(r) r^2 dr$$

normalized by the total area over the full range of radius for which the probability distribution $f(r)$ is defined, i.e. from r_0 to infinity, for the power-law distribution defined as (Follin et al., 2008, Equation C-1):

$$f(r) = \frac{k_r r_0^{k_r}}{r^{k_r+1}}$$

When multiplied by the total fracture intensity P_{32}, this gives an analytical expression for the portion of P_{32} that corresponds to the range $[r_1, r_2]$, as given in Equation C-2 of Follin (2008) based on Fox et al. (2007):

$$P_{32}[r_1, r_2] = P_{32}[r \geq r_0] \left(\frac{r_1^{2-k_r} - r_2^{2-k_r}}{r_0^{2-k_r}} \right)$$

Figure 3.12 shows the result of plotting this equation for each of the fracture sets in the final Hydro-DFN model of Follin et al. (2007a) for fracture domain FFM01, $z <$ -400 m. The plot shows clearly how the subhorizontal set (HZ) accounts for a dominant fraction of the total P32 of this model, for radii larger than about 10 m (representing distances larger than about 20 m).

A corresponding plot for the fracture sets in the Geo-DFN model (based on Table 5-3 of Fox et al., 2007, and adjusting the power-law exponents k_r using Equation C-4 of Follin, 2008) is shown in Figure 3.13. One clear difference from the Hydro-DFN, evident from this plot, is that for large fractures the subhorizontal set (HZ) does not dominate P_{32} of the Geo-DFN. Rather, it is co-dominant together with the NW- and NE- striking subvertical sets.

A comparison between the Hydro-DFN and Geo-DFN is given by plotting both sets of values together in Figure 3.14. It can be seen that the incremental fracture intensities for all of the subvertical fracture sets in the Hydro-DFN model (as represented by the symbols) plot below the values for the corresponding fracture sets in the Geo-DFN model (as represented by solid lines of the same colour; note that the Geo-DFN includes an additional, ENE set which is missing from the Hydro-DFN model). Thus for all of the subvertical sets, this geometrical constraint is quantitatively satisfied.

The values for the subhorizontal set (HZ) are difficult to see in Figure 3.14, so these are also plotted separately in Figure 3.15. This plot shows that, for subhorizontal fracture radii larger than about 200 m (corresponding to a lateral extent of about 400 m), the intensity in the Hydro-DFN model is practically equal to that in the Geo-DFN.

One obvious way to interpret this could be that, in effect, all large, subhorizontal fractures of extent greater than 400 m in the Geo-DFN model are regarded as open to flow, in the Hydro-DFN model. It should be recognized (as correctly pointed out by Follin, 2008) that the frequency of large, subhorizontal fractures might be underestimated in the Geo-DFN model, because the population of fractures (or minor deformation zones) larger than 100 m is mainly inferred from lineament data. However, it should also be recognized that the relatively high number of large, subhorizontal fractures in the Hydro-DFN is a result of adjusting parameters of a complicated network model to match borehole-testing results, without any direct observations to support the existence of such extensive, horizontal, conductive fractures at repository depths. In other words, not too much quantitative importance should be attached to the apparent close convergence of the two sets of points representing the HZ sets of the Hydro-DFN and Geo-DFN models, in Figure 3.15; both of these models should be regarded as poorly constrained for this set of features at the upper end of the size range.

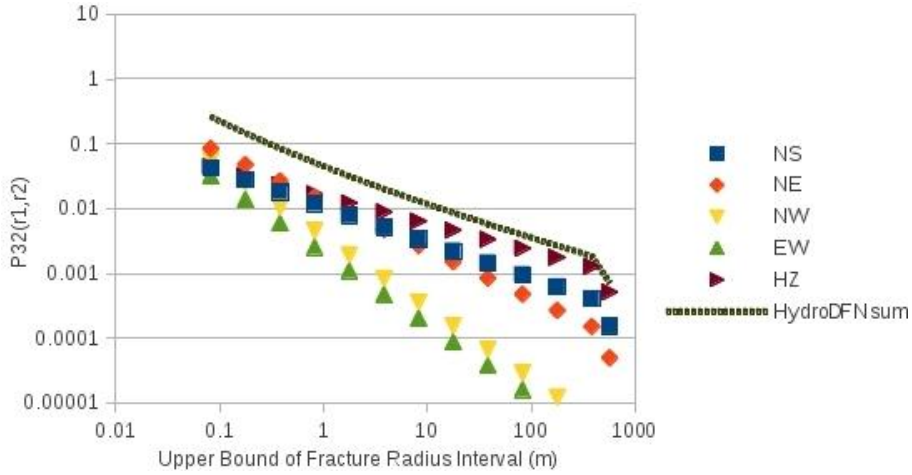

Figure 3.12: Fracture intensities P_{32} associated with discrete intervals $[r_1,r_2]$ of the fracture radius distribution, for each of the fracture sets in the Stage 2.2 Hydro-DFN model for fracture domain FFM01 for z < -400 m. Parameters for the model are taken from Table C-1 of Follin (2008). Each value of P_{32} $[r_1,r_2]$ is plotted at the radius corresponding to the upper bound r2 of the interval. The corresponding lower bound r_1 is equal to r_2 for the previous plotted value (or r_0 = 0.038 m in the case of the first interval). The sum of P_{32} $[r_1,r_2]$ over all fracture sets is shown as a dashed line in order to distinguish this more easily from the results for individual fracture sets, but note the sum is calculated and plotted for the same discrete values of r_2, rather than as a continuous function. The sharp drop for all data series for the highest value of r_2 is because this interval is truncated at the maximum defined radius, 564 m, and thus represents a shorter log-scale interval of radius than the other data points.

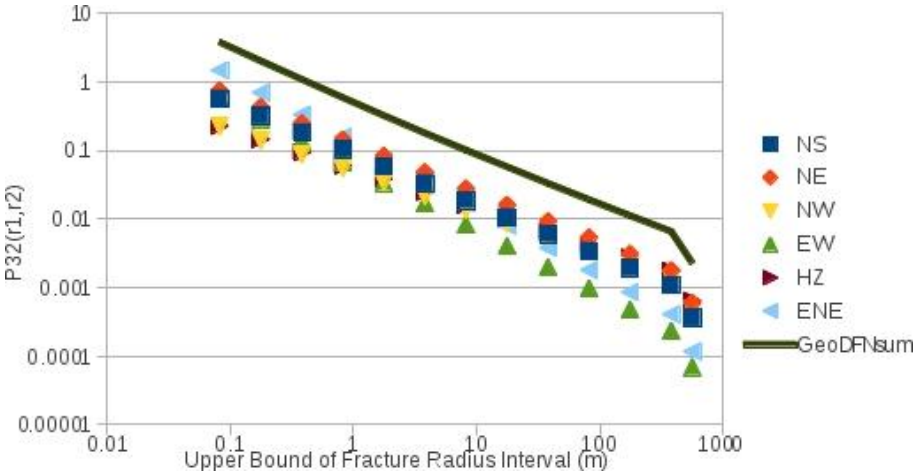

Figure 3.13: Fracture intensities P_{32} associated with discrete intervals $[r_1,r_2]$ of the fracture radius distribution, for each of the fracture sets in the Stage 2.2 Geo-DFN model for fracture domain FFM01 for z < -400 m. Parameters for the model are taken from Table 5-3 of Fox et al. (2007). Plotting conventions are the same as for Figure 3.12.

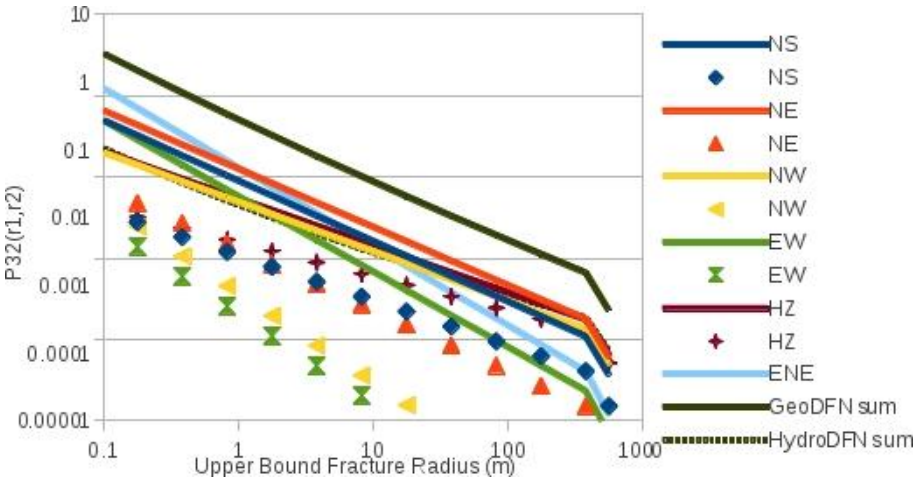

Figure 3.14: Comparison between Hydro-DFN and Geo-DFN in terms of fracture intensities P_{32} associated with discrete intervals $[r_1,r_2]$ of the fracture radius distribution, for each of the fracture sets in the Stage 2.2 Geo-DFN model for fracture domain FFM01 for z < -400 m. Parameters for the model are taken from Table 5-3 of Fox et al. (2007). Plotting conventions are the same as for Figures 3.12 and 3.13, but here continuous lines are used to show the values for individual fracture sets in the Geo-DFN model.

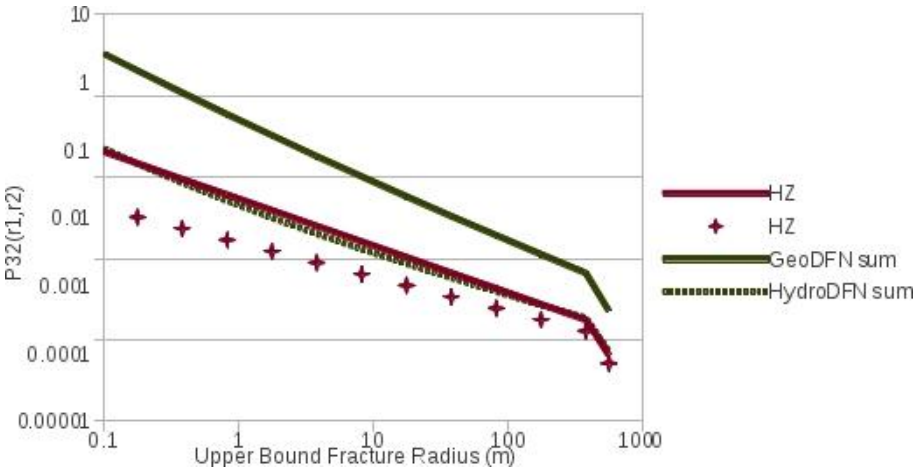

Figure 3.15: Comparison between Hydro-DFN and Geo-DFN in terms of fracture intensities P_{32} associated with discrete intervals $[r_1,r_2]$ of the fracture radius distribution, for the subhorizontal fracture set (HZ) and for the sum over all fracture sets. Parameters for the model and plotting conventions are the same as for Figure 3.14; the only difference is that the subvertical fracture sets have been omitted.

Follin et al. (2007b, Appendix C, Figure C-4) obtained a similar result for the portion of FFM01 below z = -400 m. In the shallower rock, they found that the intensity of HZ fractures in the Hydro-DFN **exceeded** the intensity in the Geo-DFN, for all fractures larger than 10 cm (effectively, all fractures in the model) in the uppermost 200 m, and for fractures larger than 10 m in the depth zone -200 m > z > -400m. The shallower depth zones are of less interest for flowrates to canisters than the rock below z = -400 m, but it is worth noting this discrepancy as further indication that the Hydro-DFN model is poorly constrained.

To summarize, the Hydro-DFN model for the fracture domain and depth interval corresponding to the near-field host rock meets this basic test of geometrical

consistency with the Geo-DFN. However, these plots give cause for concern, by highlighting the degree to which the Hydro-DFN model is dominated on large scales by extensive sub-horizontal fractures that have not been directly observed, and how the Hydro-DFN relies upon these fractures being proportionally much more likely to be open to flow, than subvertical fractures of similar size. The latter could theoretically be consistent with a reverse (thrust) faulting regime in which vertical stresses are lower than the horizontal stresses, but the gap between observable properties and the inferred model is very large.

3.3.2. Quality and uniqueness of the Hydro-DFN calibration

Comments on SKB's general approach for Hydro-DFN calibration

The approach used for calibration of the Hydro-DFN model can best be described as ad hoc or trial-and-error. This is in contrast to formal methodologies such as response-surface analysis or simpler types of sensitivity studies, in which sensitivities to the model parameters are quantified and used to search, in a rational way, for the combination (or combinations) of parameter values that give the best possible fit (or fits) to the measured data. This makes it difficult to assess whether the calibrated models represent a reasonable "best" set of parameter values for the particular mathematical model that has SKB adopted, or if they could be improved substantially through further tuning of these parameters, and/or if there are other combinations of parameter values that give equally good fits to observations.

The adjustments have been based on comparisons between measured values and averages of simulated measurements based on multiple Monte Carlo realizations of the model. The variability of these simulated measurements between realizations is not presented. This makes it difficult to assess whether the residual discrepancies can reasonably be disregarded as reflecting the stochastic nature of the model, or if these discrepancies are significant in comparison to the differences between realizations.

Taken together, these aspects:

- non-systematic trial-and-error approach,
- lack of a systematic quantification of model sensitivities to the parameters,
- lack of characterization of stochastic variation between realizations

leave a reviewer with few ways to assess the quality and uniqueness of the obtained fits, other than the same method that SKB's analysts seem to have used: subjective inspection of whether the fits were "good" or not.

An example of an apparently more systematic calibration to PFL data from Forsmark, making use of CONNECTFLOW simulations, but leading to probabilistic ranges of parameters for the transmissivity distributions and correlation to size distributions, is described briefly by Frampton (2010).

The following report referenced by Follin et al. (2007a) would appear to provide information about the sensitivity of network connectivity measures to parameters of

the Hydro-DFN model, but apparently (as of October 31, 2013) has not been produced:

> *Follin S, Stigsson M, Svensson U, 2007. Sensitivity of the connected open fracture surface area per unit volume to the orientation, size and intensity of Poissonian discrete fracture network (DFN) models. SKB R-07-28, SKB.*

According to Follin et al. (2007a), "[This] *modelling study … was not aimed at a model update, but a preparatory modelling study intended to provide some insight into new aspects of suggested procedure and the use of field data (e.g. interference tests), and therefore provide background support for the work reported here.*"

Appraisal of Hydro-DFN in terms of goodness-of-fit measures

The main part of the model fitting is essentially carried out in two steps: First the parameters of the fracture size (disk radius) distributions are adjusted to obtain what the authors judge is an adequate match of the simulated frequency of connected fractures to the frequency of PFL flow anomalies. Then the parameters of the fracture transmissivity distribution are adjusted to obtain what the authors judge is an adequate match in terms of four statistics as previously listed:

- Average total flow to the abstraction borehole over the 10 realizations.
- Histogram of flow rate to borehole divided by drawdown (notated Q/s) as an average over 10 realizations.
- Bar and whisker plot of minimum, mean minus standard deviation, mean, mean plus standard deviation, maximum of Log10(Q/s) for the inflows within each fracture set taken over all realizations.
- The average numbers of fractures within each set giving inflows to the abstraction borehole above the measurement limit for the PFL-f tests.

It can be noted that the fourth statistic used in this second step, frequency of PFL flow anomalies, is based on essentially the same data as were used to assess the fitting of the fracture size distribution model. As noted in Section 3.1.4, the calibrated Hydro-DFN model for the near-field rock over-predicts this frequency by 32% (considering all fractures), and by 50% for the subhorizontal fracture set. This appears to be a worse fit than was obtained from the first step of calibration (as reproduced graphically in Figure 3.3).

This apparent decrease in quality of fit during the adjustment of transmissivities is puzzling, since the number (intensity) of fractures in the model has not changed, nor has the fracture size distribution, so the number of "connected open fractures" should not have increased. The only possible explanation seems to be that the presence of the borehole (which is excluded from the determination of connected fractures in the first step, but is included in the flow calculations in the second step) results in an increase in network connectivity.

The idea that the borehole can increase the connectivity of a sparse fracture network was recognized by Follin et al. (2007) in their conclusions:

Based on the flow logging investigations made prior to pumping we conclude that the boreholes drilled in Forsmark increase the connectivity of the naturally flowing fractures.

but they do not seem to have recognized that this same effect could have a detrimental effect on their approach to calibrating the fracture size distribution by comparison of connected fracture frequency to PFL flow anomalies. Furthermore this result indicates that the two steps in their calibration (first size distribution, then transmissivity distribution) cannot be decoupled in the way that they proceeded; simultaneous adjustment of these distributions would be required to maintain the fit to the chosen set of statistics.

In terms of the other three measures that were used in calibration of fracture transmissivity for fracture domain FFM01, z < -400 m:

- Average total flow to the abstraction borehole is over-predicted either by 40%, or by more than an order of magnitude, depending on which reported value for "total measured Q/s" is the correct value.

- The match of simulated vs. measured histograms of flowrate to boreholes appears to be poor (the predicted values are predominantly lower, but much more strongly skewed than the measured values), particularly when considering the portions of these histograms that are above the effective measurement limit for the PFL (as discussed in greater detail by Black, 2011).

- The bar-and-whisker plots for flows to different sets give an impression similar to that from the histograms, in terms of the HZ fractures which dominate the response.

The overall impression is that there is considerable room for improvement in these fits. However, as discussed in the preceding section, it is difficult to judge the significance of the discrepancies, due to the lack of a systematic analysis of either the sensitivities to the adjustable parameters, or the variation that can be attributed to differences between stochastic realizations of the model.

The systematic underestimation of total and median values of inflows to boreholes in the histograms can be taken as a rough estimate of the potential bias resulting from insufficient calibration of the model. On this basis, it seems possible that predictions of flowrates to deposition holes based on this model could be systematically too low, by as much as an order of magnitude. On the other hand, the model predicts a few flowrates to boreholes that are half an order of magnitude higher (when normalized by drawdown) than any of the measured values. This suggests that the extreme (upper-bound) values of flowrates predicted by this model could be conservative.

3.3.3. Effects of neglecting flow channelling in Hydro-DFN calibration

SKB's Hydro-DFN model has been derived based on an implicit assumption that flow takes place uniformly through nominally disk-shaped fractures rather than

through elongated channels. As mentioned above (Section 3.3.1), concerns about this approach were raised by SSM's INSITE review group (INSITE, 2008):

> *"Where previous versions of the Hydro-DFNs were derived from the Geo-DFNs, ensuring geometric consistency, the current Hydro-DFNs have loosened the reliance by calibrating size-distribution parameters directly to flow anomalies observed with the Posiva Flow Log (PFL). INSITE considers that the relationship of Hydro-DFN geometric parameters to PFL anomalies is poorly constrained. Alternative conceptual models, for instance channelised fractures, could give rise to Hydro-DFN models that match the data equally well, but have very different implications for geochemical stability of the near-field and radionuclide transport in the far-field."*

Channelization and aperture variation are recognized in SKB's conceptual description for transport modelling, but are not accounted for in the connectivity analysis and calibration approach that underlies the Hydro-DFN. Calibration of a Hydro-DFN model, following SKB's line of reasoning but taking channelization into account, would presumably lead to different parameters for the size distribution of subhorizontal fractures.

As part of the site descriptive modelling for a similar site in Finland, Posiva Oy has considered a Hydro-DFN model variant which assumes that all fractures in the Geo-DFN model for that site (Fox et al., 2012) are transmissive over only a fraction of their area. This model variant, as developed by Hartley et al. (2012) assumes an unstructured random distribution of the transmissive areas. The results as presented by Posiva (2012, p. 722) show slightly increased percentages of deposition holes that are connected to flowing networks, in comparison to models similar to those considered by SKB for Forsmark. The differences in connectivity are modest (1% to 5% in comparison with Posiva's base case). Conceivably a more structured (spatially correlated) distribution of transmissivity within each fracture plane could lead to more significant differences.

Alternative calculation cases that could give rise to stronger channelling than the model variant developed for Olkiluoto by Hartley et al. (2012) could certainly be envisioned, but these are best dealt with in Section 4 of this technical note, concerning alternative conceptual models.

4. Review of alternative conceptualizations and parameterizations

4.1. SKB's presentation of alternatives

The following three subsections summarize SKB's presentation of alternative conceptualizations, alternative parameterizations, and general discussion of uncertainty relating to the Hydro-DFN models.

4.1.1. SKB's discussion of alternative conceptualizations

The SR-Site main report and supporting documents present no alternative hydrogeological conceptualizations of the near-field host rock that are independent of the Hydro-DFN model. Where alternative conceptual models are discussed, these refer to alternative methods for simulating flow and transport through models that are upscaled from the Hydro-DFN model, namely:

- Simulations of flow and transport for temperate conditions using the channel-network model CHAN3D (Liu et al., 2010), which is conceptualized as a regular, orthogonal grid of conductors. As described in the SR-Site main report (p. 353), this model "is parametrised using the statistics of block-conductivity values resulting from up-scaling of the original hydrogeological DFN model" and thus ends up with a connectivity structure that is basically the same as the upscaled ECPM model (except that flow is constrained to the rectilinear grid rather than being allowed to flow at an angle to the calculation grid); the main difference is in terms of solute mixing at vs. between junctions in the grid. As noted in TR 11-01 (p. 353) it yields very similar median values of the performance measures (flowrates to deposition holes and transport resistance), though less spreading of results than in the CONNECTFLOW simulations based directly on the Hydro-DFN model. The CHAN3D application (Liu et al., 2010) does use an independent estimate of the flow-wetted surface parameter a_r for calculating transport resistance, based directly on observed fracture frequency in boreholes, rather than a_r values calculated by the Hydro-DFN model, but this parameter does not enter into calculations of flowrates to deposition holes.

- Continuous porous medium (CPM) models are mentioned as an alternative conceptual model in reference to previous calculations for the SR-Can safety assessment, noting that an alternative multi-component CPM formulation provided more favourable results in contrast to an ECPM/DFN model (Data Report, p. 342).

SKB does not seem to recognize any conceptual uncertainties related to the assumption of a DFN based on disk-shaped fractures, with uniform transmissivity in

each fracture, except with regard to the effect of aperture variability on transport resistance as discussed in the Main Report, p. 354:

> *The calculated flow-related transport resistance (F) values can be used unmodified in subsequent radionuclide transport and oxygen penetration calculations. In SR-Can, F values were divided by a factor of ten to account for channelling. In SR-Site no such channelling factor is used based on motivations provided in the Radionuclide transport report. First, fracture-to-fracture variability is generally larger than within-fracture variability in aperture. Second, fluid can only enter and leave fractures on a limited area, significantly constraining the meander of flow paths. Third, substantial portions of the non-contacting fracture surface area outside of the dominant flow channels may still be accessible by diffusion within the fracture pore space and thus provide additional surface area for radionuclides to interact with the rock matrix.*

These arguments are reasonably well supported by the work of Painter (2006) and Crawford (2008). However, they do not relate to the issue of network connectivity (percolation) for flow models.

The Data Report section on conceptual uncertainties in the hydrogeological model (Data Report p. 329, Section 6.6.6) discusses only:

- The same conceptual constraints on open fractures as a subset of all fractures, connected open fractures as a subset of open fractures, and PFL anomalies as a subset of connected open fractures which are the basis for the consistency check of the Hydro-DFN model as discussed in Section 3.3.1 of this review;
- The "tectonic continuum" assumption of a power-law size distribution spanning the full range of fracture sizes (stated as a key assumption without mentioning alternatives or reasoning);
- Assignment of fracture transmissivity (here SKB gives a very brief description of the transmissivity calibration approach which is discussed in Section 3.1 of the present review, and once again mentions the four statistics that have been discussed in Section 3.3.2, Appraisal of Hydro-DFN in terms of goodness-of-fit measures).

No alternative models or parameterizations are suggested for evaluating these uncertainties, and no other conceptual uncertainties or alternatives are mentioned.

On p. 339 of the Data Report, the judgement of the SR-Site team regarding **Conceptual and data uncertainties** is stated as follows:

> *The sources of uncertainty of all parameters are adequately described and quantified. It is noted that the hydrogeological discrete fracture network model is associated with conceptual uncertainty as described above. This relates both to the geometrical description of the network, but maybe even more importantly to the hydraulic parametrisation, specifically the assumed fracture size-transmissivity correlation model, see Table 6- 74* [the table which gives the parametric form of the correlated, uncorrelated, and semi-correlated models that were evaluated for the Hydro-DFN].

Thus SKB does not acknowledge the possibility of any discrete conceptual models for flow, outside of the DFN concept based on disc-shaped fractures with uniform transmissivity in each fracture. No reference is made to work regarding evidence for channelized flow in the general scientific literature (e.g. Tsang and Neretnieks, 1998) or to SKB's previously commissioned work on alternative channel network models (Black et al., 2006; Black et al., 2007).

4.1.2. SKB's treatment of alternative parameterizations

In addition to the base model simulation which allows comparison between homogeneous vs. stochastic variation of transmissivity in the HCDs, hydrogeological variants evaluated in CONNECTFLOW modelling of the temperate period (Joyce et al., 2009, Chapter 5 with results given in Section 6.3) included:

- Alternative DFN transmissivity-size relationships
- Possible deformation zones
- Unmodified vertical hydraulic conductivity
- Extended spatial variability
- Tunnel variants
- Effect of boreholes

The last two of these (tunnel variants and effects of boreholes) consider the effects of engineered structures on connectivity and flow through the fractured bedrock, and do not address uncertainty in the parameterization of the bedrock itself. The other variants do concern parameterization of the bedrock, and are discussed in relation to uncertainty in the Hydro-DFN model and consequences for flows to deposition holes, in the following paragraphs.

In addition it should be mentioned that the SR-Site calculations considered a parametric variant concerning

- Correlation of fracture aperture to fracture transmissivity

The site-descriptive model calibration stage also considered sensitivity cases for upscaled (ECPM) model parameters that affect transport:

- Kinematic porosity
- Flow wetted surface per unit rock volume

These variants do not affect the predictions of groundwater flowrates to deposition holes, but affect the calculation of groundwater velocities, radionuclide transport, and groundwater-rock interactions.

The calibration of the site-descriptive model also considered alternative vertical divisions of the fracture domain FFM01, with either one or two distinct statistical descriptions for the Hydro-DFN of the model for the bedrock shallower than z = -400 m. The SR-Site Data Report (p. 342) states: "*Within the discrete fracture*

network (DFN) conceptual model, results proved to be sensitive to the chosen fracture size-transmissivity model, and to the implementation of a multi-component DFN representation; that is to a model with different DFN statistics in different parts of the domain." However the SR-Site Main Report (p. 354) states, "[*T*]*he other SDM-Site related variants [aside from the fracture transmissivity vs. size models] do not warrant further consideration in the assessment.*" Thus alternative divisions of the Hydro-DFN in terms of depth domain apparently were not considered to warrant propagation to safety calculations.

Homogeneous vs. stochastic variability of transmissivity in the HCDs

The fact that a single realisation of the HRD (r1) was used in combination both with the "homogeneous HCD" model and one realization of the "stochastic HCD" model allows comparison of these two models of HCD transmissivity variation. Based on the results presented in Figure E-22 of Joyce et al. (2009), the effects of "homogeneous" vs. "heterogeneous" HCDs on near-field flows appear to be insignificant.

Variation between stochastic realizations is more significant, with one realization yielding roughly twice as many canister positions with flux values Ur > 0.001 m/s than any of the other nine realizations, about four times as many canister positions with Ur > 0.01 m/s, and what appears to be a similar ratio for the number of canister positions with Ur > 0.1 m/s. This indicates that heterogeneity in the HRD model has a more significant impact on near-field flow distributions than heterogeneity in the HCDs.

Alternative DFN transmissivity-size relationships

Variants regarding the assumed parametric relationship between fracture transmissivity and fracture size have received the most attention in SKB's calculations for SR-Site. The *T* vs. *r* variants considered by Joyce et al (2009) are the same uncorrelated and (perfectly) correlated models described in Section 3.1.3 that were suggested and tested by Follin et al. (2007a; 2007b; 2008), as alternatives to the "semi-correlated" model which is treated as part of the central case for SR-Site.

As stated in the SR-Site Main Report (p. 354), "*the results for these variant cases [as studied in SDM-Site] indicate that the performance measures of the semi-correlated relationship utilized in the hydrogeological base case model in general are more favorable than the other two correlation models*," so these were propagated through the safety assessment calculations for analyses of buffer erosion, canister corrosion and radionuclide transport.

The Main Report states (p. 609) that the semi-correlated variant (combined with the SR-Site model for buffer erosion) is seen as a central corrosion variant, because "*[t]he semi-correlated DFN model is more compatible with site data than the other two cases since its description of the relation between fracture size and transmissivity is most consistent with observations …. The remaining combinations of hydro DFN models and erosion cases are seen as illustrative cases providing bounds on uncertainties in the aspects of corrosion they represent.*"

As further justification for propagating these particular variants, the Data Report (p. 335): contains a statement that:

"The hydraulic calibration (parameterization) of the generated DFN realizations reveal that all of the tested transmissivity models give reasonable matches against the four 'goodness of fit' statistics discussed in Section 6.6.6. Hence, none of the tested transmissivity models is discarded in SR-Site. However, the semi-correlated transmissivity model is advocated to be the most realistic of the three models attempted. For SR-Site, it is suggested that the correlated and uncorrelated transmissivity models should be tested as variants."

Based on the results discussed in Section 3.1, it is arguable whether any of these models gave convincing enough matches to the four statistics mentioned, to represent a particularly realistic model of the repository host rock. However, the fact that the correlated and uncorrelated cases gave less favorable results than the semi-correlated case is a compelling reason to propagate these cases to safety assessment, even if they do not fully bound the uncertainty related to the Hydro-DFN description of the host rock.

The results of Joyce et al. (2010) indicate that Darcy flux to deposition holes is "*dependent on the chosen transmissivity-size relationship, with up to about half an order of magnitude variation between variants*" (SR-Site Main Report, p. 350). Figure 4.1 shows the key results in terms of flowrates to canisters for the central corrosion case and the two Hydro-DFN transmissivity/size model variants. It can be seen that both the "uncorrelated" and "correlated" Hydro-DFN models lead to a prediction of a higher number of advective positions, and numbers of failed canisters, for time scales of 100,000 to 1,000,000 years.

Despite that the correlated and uncorrelated variants gave less favorable results, and represent distinctive cases (in the sense that different terms in the mathematical form of the semi-correlated model have been effectively been set to zero, before adjusting the other two parameters to improve the fit to observed hydrogeological data), there is no certainty that these represent "end-member" cases.

Finally the following puzzling statement should be noted regarding the Hydro-DFN fracture size distribution (SR-Site Data Report, p. 323):

"*As the repository layout was not part of the site-descriptive modelling, the fracture size distribution has been modified in the groundwater flow modelling activities being part of SR-Site, in order to account for the repository system impact on how discrete fractures are connected."*

A description of a modification in the size distribution to account for repository system impacts has not been found in any of the hydrogeological modeling reports considered for this review, so perhaps this is just a mistake in phrasing.

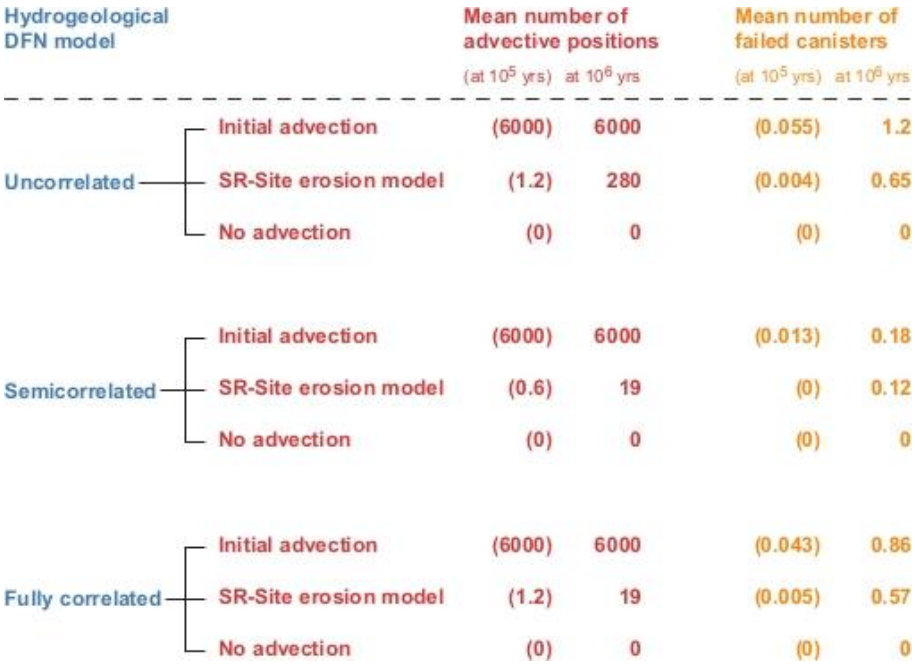

Figure 4.1: Reproduced from SR-Site Main Report, Figure 12-18. Mean number of advective deposition positions and mean number of failed canisters for the calculation cases identified as relevant for the corrosion scenario.

Possible deformation zones

The hydrogeological model variant that considers "possible deformation zones" (PDZs) includes four deterministic HCDs which are treated deterministically (Selroos & Follin, 2010, p. 59):

> *"Forty-three possible deformation zones (PDZ) were identified in the single-hole geological interpretations. /Follin et al. 2007b/ established that only ten of these corresponded with a hydraulic test above the detection limit. Of these, six were found to be gently dipping zones in the top 150 m of bedrock and considered to be already represented by the implementation of the near-surface sheet joints, leaving four PDZs above the hydraulic detection limit at or close to repository depth."*

As depicted in Figure 4.2, the two larger PDZs apparently have horizontal extents of about 1000 m, while the two smaller PDZs have horizontal extents of about 500 m.

Thus the two smaller PDZs are apparently within the size range that is represented by the Hydro-DFN model. Thus their inclusion provides some insight into the sensitivity of the Hydro-DFN model to including a few additional conductive fractures, in the upper end of the size range. However in contrast to large fractures in the Hydro-DFN, the PDZs are represented as having depth-dependent, spatially variable hydraulic conductivity.

From the color scale in Figure 4.2, the hydraulic conductivities assigned to these features at repository depths are in the range 10^{-10} m/s to 10^{-8} m/s. The widths assumed for this variant are not listed in the main hydrogeological modelling reports, but assuming a width of 10 m, this corresponds to a transmissivity range 10^{-}

^{9} m^2/s to 10^{-7} m^2/s. By comparison with Figure 3.4, this range is about an order of magnitude higher than the transmissivities assigned to similar-sized fractures in the central ("semi-correlated") variant of the Hydro-DFN model for similar depths, but about the same as for the "correlated" variant.

The results for three realizations of the hydraulic conductivities for PDZs in this variant, as reported by Joyce et al. (p. 99-100), show no significant effect on the distribution of flows to deposition holes, relative to the variation that is seen between stochastic realizations of the hydrogeological base case model. However, an effect is noted on the tail of the Fr distribution for the Q3 release path, which (as noted by Joyce et al.) implies the existence of one or several indirect release paths via intersection between the PDZs and repository tunnels, rather than a direct intersection with a deposition hole (apparently no direct calculation to check for such intersections was made). Thus the lack of sensitivity in terms of flowrates could just be an artifact of the exact position of the PDZs, relative to the deposition hole positions.

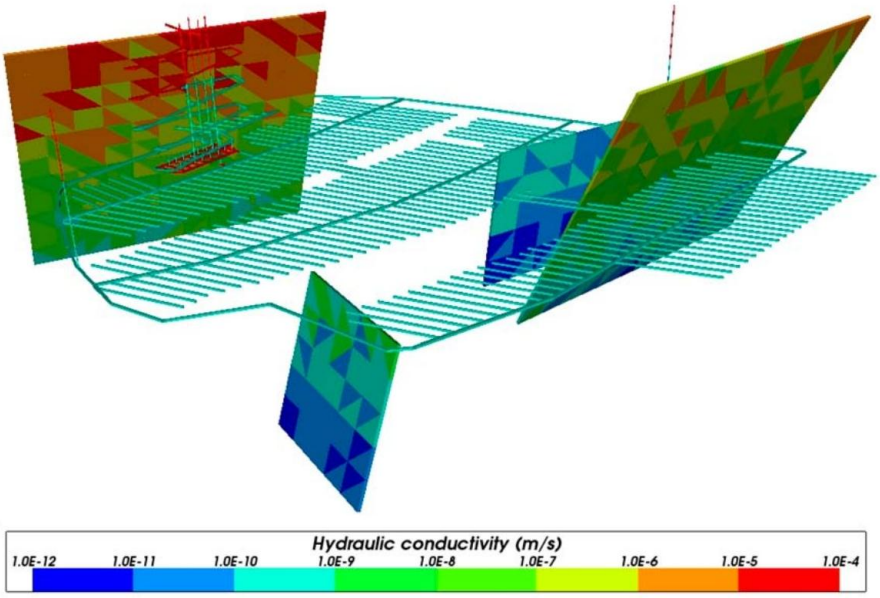

Figure 4.2: (reproduced from Joyce et al., 2009, Figure 5-1) Possible deformation zones (PDZs) included in the model variant of the same name, depicted in relative to the repository structures. Hydraulic conductivities for a particular stochastic realization are indicated by the color scale. No length scale or indication of perspective is given in the original figure, but approximate scales may be estimated considering that the shafts leading to from the surface to the repository central area are approximately 465 m long.

Unmodified vertical hydraulic conductivity

The motivation for the "unmodified vertical hydraulic conductivity gradient" variant was explained by Selroos and Follin (2010, p. 60) as follows:

> *"During the calibration and confirmatory testing of the SDM base model simulation, the vertical conductivity of the HRD above an elevation of –400 m was reduced by a factor of ten in order to provide a better fit to chemistry and interference test data. This was also used for the ECPM in the hydrogeological base case for SR-Site. However, no corresponding change was made to the properties of the fractures in the DFN representation of the HRD, leading to a*

possible inconsistency in flows between the DFN and CPM in the site-scale model.

"This variant removes the modification of the vertical conductivity of the ECPM used in the regional and site-scale models."

In other words, the increased vertical hydraulic conductivity K_v in the upper part of the hydrogeological base case model was not applied to the entire volume of the site-scale model above z = -400 m, but only to the part of that volume which was represented by an ECPM or CPM. This is illustrated by the shaded areas in Figure 4.3. The effect is that the central part of the site-scale model above the repository (where the DFN representation was used) has, on average, lower effective K_v than the surrounding parts, and this is not consistent with the regional-scale representation.

The effect of the "unmodified vertical hydraulic conductivity" variant was thus simply to reduce the K_v of this layer to the values that were originally obtained by EPCM upscaling of the Hydro-DFN model.

Hence this variant is mainly to correct an upscaling inconsistency between different domains of the models, rather than to assess uncertainty in the Hydro-DFN. As the change is applied mainly to portions of the bedrock that that are outside the footprint of the repository, and only to the upper part of the rock, it could be guessed that it will not have a significant effect on flowrates to deposition holes. Indeed, the results (as given by Joyce et al., 2009, Figure E-43) are practically identical to those for the base case.

A more consequential variant for testing Hydro-DFN parametric uncertainties could have been to increase the transmissivities of the subvertical Hydro-DFN fractures in the upper part of the site-scale model, to make these more consistent with the enhancement of K_v in the ECPM and CPM portions. This would also test the effect of varying the model properties within the footprint of the repository, where they are more likely to have a measurable impact on near-field flows.

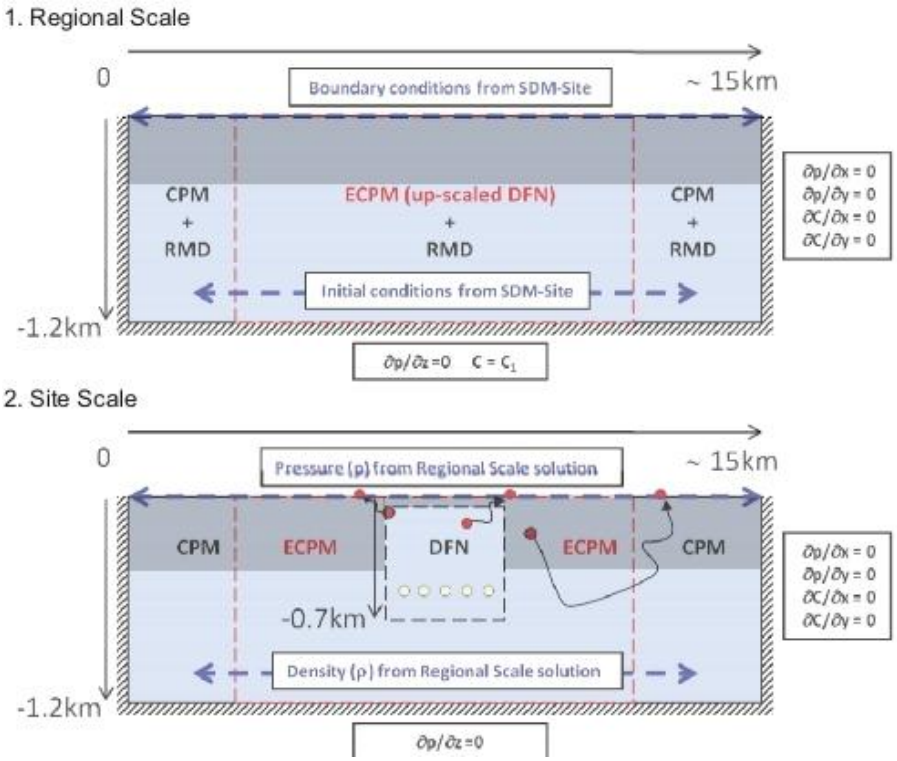

Figure 4.3: Illustration of the regional and site modelling scales used in CONNECTFLOW modeling for the temperate period, based on Selroos and Follin (2010, Figure 3-6), but with darkened areas in the upper 400 m of ECPM and CPM volumes to show the volumes within which the vertical component hydraulic conductivity was increased by a factor of 10 during calibration for the SDM-Site model.

Extended spatial variability

This variant replaces the homogeneous and isotropic CPM in the outer portions of the base-case model with a heterogeneous ECPM, based on upscaling a separate Hydro-DFN model (Öhman and Follin, 2010) that was derived based on ongoing investigations related to a shallow, low- and intermediate-level radioactive waste facility (the SFR) which lies to the north of the proposed location of the deep spent-fuel repository. In addition, the area of the DFN in the site-scale model was extended northwards beyond the Singö deformation zone.

Like the “reduced vertical conductivity” variant, this variant does not involve changes to the Hydro-DFN model for the host rock for the repository deposition tunnels, or for the rock directly above the tunnels. Joyce et al. (2009) note effects on the spatial distribution of discharge points at the surface, in the direction toward the Singö deformation zone. However this variant has very little influence on flowrates to deposition holes.

Fracture aperture-transmissivity relationships

Alternative correlations between fracture aperture and transmissivity are discussed on p. 335-336 of the Data Report, and seven alternative models of this correlation are plotted in Figure 6-66, of which two are chosen for evaluation. However, aperture is only used within SKB's approach for calculating transport resistance

(using Equation 6-18 of the Data Report), and does not affect calculations of flowrates to deposition holes.

4.1.3. SKB's discussion of DFN model uncertainties

This section summarizes SKB's presentation of uncertainties related to the Hydro-DFN model, apart from those considered in the variants mentioned in the preceding sections. According to the SR-Site Main Report (p. 301):

> "*General uncertainties related to the hydrogeological modelling, specifically the use of discrete fracture network (DFN) modelling within hydrogeological modelling, are discussed in more detail in the Data report (Section 6.6) and in / Selroos and Follin 2010/.*"

The SR-Site Main Report (p. 353) also states:

> "*General uncertainties of the results presented in this section are related to the derived hydrogeological discrete fracture network (DFN) model used in the hydrogeological base case. A comprehensive discussion of these uncertainties, including the relation between the hydrogeological DFN and geological DFN models, is presented in the Data Report*."

Considering Section 6.6 of the SR-Site Data Report, the main sections that discuss uncertainties are Section 6.6.6 ("Conceptual uncertainty") and Section 6.6.7 ("Data uncertainty due to precision, bias, and representativity"). However, as noted previously, Section 6.6.6 simply mentions the logical geometric constraints on intensities of connected fractures vs. open fractures vs. all fractures in the DFN conceptual model, and then (very briefly) describes the criteria for calibration of the three alternative transmissivity-size relationships which have already been discussed in the present technical note.

Section 6.6.7 describes several sources of uncertainties:

- Limited precision in position of PFL anomalies along boreholes;
- Uncertainty in assignment of fracture geometrical properties to flow anomalies due to this limited precision as well as occasional uncertainty in deciding which fracture a flow anomaly represents;
- Detection limit of the single-hole hydraulic testing methods in terms of specific capacity which affects the measured frequency of flow anomalies;
- Uncertainty regarding what a given hydraulic test represents (hydraulic choke and specific capacity concepts).

The authors consider that the last issue mentioned is dealt with by the calibration approach, which includes forward-modelling simulation of the types of network effects that could lead to "hydraulic chokes." For the other sources of uncertainty, there is no discussion of how to propagate the consequences of (1) errors in the measured frequency of flow anomalies, or (2) mistaken assignment of the wrong fracture geometric properties to flow anomalies (e.g. such as by sensitivity cases considering variations in the conductive fracture intensity for different fracture sets).

Spatial heterogeneity of fracture intensity spanning roughly an order of magnitude, for both “open” fractures and PFL flow anomalies, is indicated by plots showing the range of Terzaghi corrected fracture frequency among boreholes (Data Report Figure 6-64). However, the text of this section discusses only the mean value, and the fact that this mean value is very low for the rock below -400 m. No comment is given on the implications of the spatial heterogeneity which is evident from the plot, in terms of the Hydro-DFN model.

The corresponding part of the Data Report (Section 6.3.6) that deals with uncertainties in the Geo-DFN model gives much more attention to conceptual uncertainties in fracture size-intensity relationships and spatial heterogeneity in fracture intensity. Conceptual uncertainties identified in a formal inventory of uncertainty by (Fox et al. 2007) include, for example:

- Validity of the Tectonic Continuum hypothesis as opposed to the OSM+TFM or r0-fixed conceptual models;
- Choice of cut-off between large fracture and minor deformation zone[s] (affects the OSM+TFM alternative);
- Euclidean vs. fractal scaling of fracture intensity [this issue is assessed as minor]; and
- Whether the lack of clustering (i.e. Poissonian spatial arrangement) observed in outcrop and borehole data carries over to the large-fracture and MDZ size range within the Forsmark local model volume.

The Geo-DFN models mentioned by acronym here (OSM+TFM or r_0-fixed) are described on p. 244 of the Data Report.

The magnitude of the various conceptual and mathematical uncertainties in the geological DFN model were assessed by Fox et al. (2007) in terms of fracture intensity (P_{32}) ratios between pairs of alternative models, for two different size ranges (0.5–564.2 m and 28–564.2 m). These P_{32} ratios are summarized in Table 6-31 of the Data Report, as reproduced below in Table 4-2. The largest conceptual uncertainty, in terms of its effect on P_{32}, is seen to be the method by which the fracture size distribution is parameterized.

Table 4.2: Summary of key conceptual uncertainties and their expected impacts on downstream models (reproduced from Table 6-31 of the SR-Site Data Report).

Uncertainty	Magnitude	Comments
Fracture size conceptual model	0.3–3.0	Varies significantly as a function of fracture set and fracture domain
Boundary between OSM and TFM	0.6–0.9	Specifying a boundary between OSM and TFM reduces the total fracture intensity by approximately 1/3
Euclidean vs. fractal intensity scaling	0.82–1.16	Minor impact, especially on subhorizontally-dipping fractures and MDZ
Use of size data from surface (FFM02) to parameterize domains at depth	0.3 – 0.7	This uncertainty promoted to full-fledged model (r_0-fixed); results in significantly lower intensity in the MDZ size range (28 – 564.2 m)
Fracture intensity as a function of rock domain	0.5 – 2.0	Impact is greatest for minor rock types such as amphibolite and pegmatite
Fracture intensity as a function of depth	~0.9 – 1.05	Varies significantly as a function of fracture set and fracture domain

4.2. Motivation of the assessment

Due to the importance of the Hydro-DFN for the repository host rock (particularly fracture domains FFM01 and FFM06 at depths greater than 400 m) for SKB's predictions of flow to deposition holes, any viable alternative conceptual models or parameterizations need to be considered, particularly in terms of their potential impacts on the number of deposition holes that encounter significant flows, and the distribution of magnitudes of such flows.

4.3. The Consultants' assessment

The evaluation of alternative conceptualizations and uncertainties given by SKB spans only a very limited range of the topics that should have been considered. The Hydro-DFN model developed by SKB neglects potentially significant sources of uncertainty, as well as evidence for spatial variability which is recognized in the Geo-DFN models for SR-Site.

The calibration of the Hydro-DFN for the bedrock at repository depth is based on a spatially very limited dataset (i.e. flow anomalies in boreholes which are very widely spaced in comparison to most of the considered size range of stochastic fractures, plus a small number of "representative" geochemical samples. The fits obtained (as discussed in Section 3) are not especially convincing. These considerations suggest a high likelihood that alternative models of the flow system, as well as alternative parameterizations, could produce at least equally convincing fits to the data.

For example, consequences of the following alternatives could be considered:

- DFN model with statistically heterogeneous fracture intensity as recommended by SKB's Geo-DFN analysts (Fox et al., 2007);

- DFN model with clustering due to spatial correlation of small-scale fractures to large-scale fractures (demonstrated to be consistent with the Forsmark data, in a previous study for SSM by Geier, 2011c);

- Channelized DFN models (Nordqvist et al., 1992);

- Sparse channel network model as formulated in a previous alternative-model study commissioned by SKB (Black et al., 2006; Black et al., 2007).

As these alternatives have not been explored in any degree by SKB's SR-Site analysis, their potential for producing significantly different results in terms of flows to deposition holes are discussed in the following subsections.

4.3.1. Heterogeneous-intensity DFN models

The Geo-DFN for the target volume at Forsmark includes a description of statistical heterogeneity in fracture intensity (Fox et al., 2007), represented as a gamma distribution which was tested for block scales of 6 m and 30 m, and was found to be applicable for those scales. Other block scales in the range of interest (e.g. the 20 m and 100 m scales which were used for ECPM upscaling in the SR-Site hydrogeological simulations) were not tested, but it should be expected that some degree of P_{32} heterogeneity is also present on those scales.

Figure 4.4 shows the quantiles of the gamma distributions of P_{32} for each of the fracture sets in the Geo-DFN model for FFM01. The 90th percentiles for P_{32} are typically at least double the median values which have been used for homogeneous-P_{32} models in SR-Site. This model implies that 10% of blocks on a 30 m scale will have fracture intensities at least twice as high as the "average" rock in FFM01.

Considering that the fractures in FFM01 are interpreted as being very sparse, and that the population of open or partly open (i.e. potentially transmissive) fractures is even more sparse, this heterogeneity is potentially very significant for percolation in the Hydro-DFN. A separate review for SSM (Black, 2011) has pointed out that the total P_{32} of 0.63 m^{-1} of open (transmissive) fractures in SKB's Hydro-DFN model, for FFM01 at depths below -400 m, is just barely above the percolation threshold of 0.6 m^{-1} that could be calculated based on the classical investigations of Robinson (1984).

A DFN model with the same average P_{32}, but with gamma-distributed, heterogeneous variation of this parameter on the block scale, will have a substantial fraction of blocks that are well above the percolation threshold, as well as a corresponding fraction that are well below the percolation threshold, and are likely to be entirely non-conducting.

This type of model can be expected to lead to a binary flow system, in which flow is focused through the parts of the rock where fractures are more concentrated, with large volumes of non-percolating rock in between. In portions of the rock with P_{32} well above the percolation threshold, small-scale fractures would frequently form parts of connected networks. This differs from the Hydro-DFN model used in SR-

Site, in which connections on the scale of ECPM blocks or larger are almost entirely dependent on a few, very large fractures.

A full quantitative assessment of the effects on flowrate distribution, for a Hydro-DFN that accounts for the degree of heterogeneity that has been demonstrated by Fox et al. (2007) for the Geo-DFN, would require:

- Calibration of a fracture transmissivity distribution based on the available borehole testing data (independent of the SDM-Site calibration which was based on a uniform- P_{32} model), and then

- Simulation of flowrates to deposition holes in a site-scale network model.

Without going through this type of calibration and simulation exercise, it is difficult to estimate effects on the distribution of flows to deposition holes. However, it seems likely that the main effect would be to focus flow through fracture networks in a few parts of the rock volume, but those flowing networks would tend to be less strongly dominated by extensive single fractures, compared with the SR-Site Hydro-DFN. The consequences of such a system might include an increase in the number of deposition holes with flowrates in the upper part of the range predicted by the SR-Site base case, but not necessarily more extreme values to individual deposition holes.

One further implication of this type of heterogeneous- P_{32} model is that deposition holes with significant fluxes would tend to be clustered together in portions of the repository which have higher-than-average P_{32}. Canister positions exposed to high fluxes would tend to be clustered in space, increasing the potential for multiple canister failures to be likewise clustered.

In these parts of the repository, small-scale fractures as well as large-scale fractures could tend to be part of flowing networks. Hence avoidance of large fractures (using the proposed EFPC criteria) might not yield such favourable of results for avoiding high-flux deposition holes, as has been suggested based on simulations of the SR-Site Hydro-DFN model (Svensson and Follin, 2009). On the other hand, geological mapping in tunnels could help to indicate zones of higher-than-average fracture intensity, which (if transmissive fractures are a consistent fraction of all fractures) could indicate less favourable sections of the repository in terms of flow.

The implications of the SR-Site Geo-DFN model in terms of the EFPC criteria will be explored further based on numerical calculations, as an ongoing, supplementary part of this review task which is aimed at confirming SKB's calculations of utilization factors for deposition tunnels. A quantitative assessment of the consequences of heterogeneous P_{32}, based on the recommendations of Fox et al. (2007), should be possible as one outcome of those calculations.

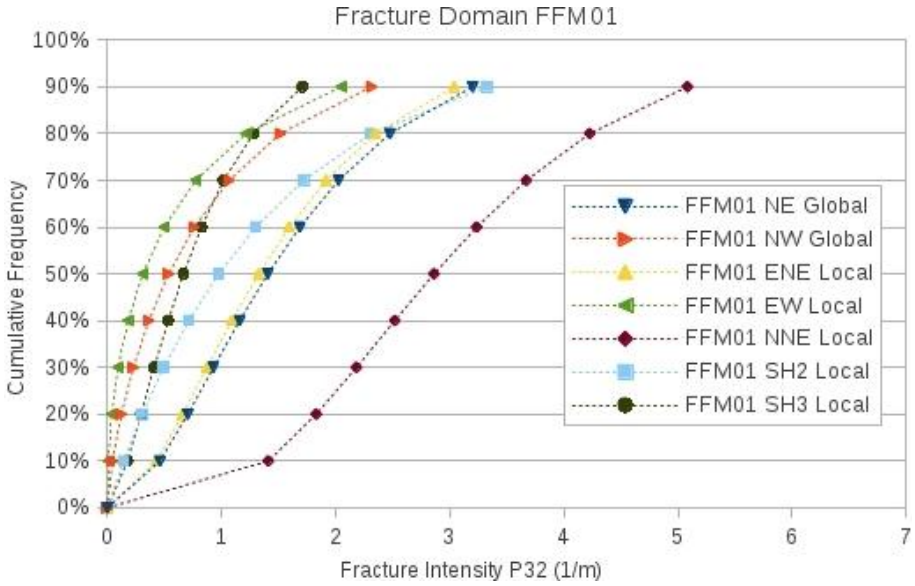

Figure 4.4: Quantiles of fracture intensity P32 of fracture sets in fracture domain FFM01, calculated based on gamma distribution parameters given by Fox et al. (2007, Table 4-96).

4.3.2. DFN clustering around minor deformation zones

An alternative DFN model with non-uniform fracture intensity has been derived for the Forsmark site based on an analysis of fracture clustering along boreholes (Geier, 2011c). This model is based on the common observation from structural geology that extensive brittle structures in crystalline rock tend to be minor deformation zones rather than single discrete fractures (as was recognized in SKB's geological site investigations at Forsmark and Laxemar, and the discussion of conceptual uncertainties by Fox et al., 2007), and that smaller-scale fractures tend to be clustered in a "halo" around these minor deformation zones (referred to as MDZs, in SKB's site investigations).

As detailed by Geier (2011c), a "halo" model for average fracture intensity decaying as an exponential function of distance h from the nearest deformation zone was postulated:

$$\overline{P}(h) = P_{\infty}\left[1 + ae^{-\alpha h}\right]$$

where:

P_{∞} = mean fracture intensity of the background rock (far from the influence of any deformation zone)
a = dimensionless fitting parameter representing the increase in fracture intensity close to a deformation zone;
α = fitting parameter characterizing the decay of fracture intensity with distance [units of inverse length]

For fracture domain FFM01, a least-squares fit of this model to one-dimensional fracture intensity (P_{01}, i.e. fracture frequency) data from boreholes yielded $a = 6$ and $\alpha = 0.1$ m^{-1}. In rough terms and on average, this implies that the fracture intensity at the edge of a deformation zone exceeds the background fracture intensity by about a factor of six, and this excess fracturing diminishes by a factor of about one third for every 10 m of distance.

It should be noted that the scatter of results around this model was very substantial, and fracture frequencies exceeding the background value by a factor of more than 10, as well as many zero values, were common for the first 15 m of distance from the nearest deformation zone. The fitted model does not capture this variability, but represents the observed trend.

Simulations of flow through a hypothetical repository at Forsmark were carried out using a multi-scale discrete-feature model (DFM) based on the same large-scale hydro-structural model as employed in SR-Site, and an upscaled representation of rock-mass hydraulic conductivity in the far-field, but with an explicit DFN representation around the repository tunnels. The same type of model set-up was used to simulate flow with a DFN component based directly on the Hydro-DFN parameters given by Follin (2008), in order to compare the consequences of a clustered vs. uniform fracture intensity. Apart from spatially varying fracture intensity, the same fracture set parameters were used in both model variants (uniform-P_{32} and "halo" variants). Thus the fracture transmissivity distribution was not recalibrated for the halo model.

The resulting flowrate distributions to deposition holes are shown in Figure 4.5, comparing two realizations of the base case (based on SKB's SR-Site model) with two realizations of the halo model. These flowrate distributions include both deposition holes that connect to the far-field network via discrete fractures in the DFN (Q1 path), and deposition holes that connect via an assumed EDZ in the base of the tunnel (Q2 path).

Both realizations of the halo model in Figure 4.5 show an increase in the proportion of deposition holes that carry flows higher than 100 litres/year, relative to the base case DFM simulations. In terms of these higher-flow holes, there is also high variability between realizations of the exponential-halo model. At the low end of the flow range, the differences with the base case are minor relative to the differences between realizations.

The main effects of possible significance for safety calculations seen from thus that the halo model variant yields:

- 1 to 2 orders of magnitude increase in flowrates for a small percentage of canister positions;
- Strong effect of stochastic realizations.

This alternative model for clustering of fractures within the DFN was also evaluated in terms of consequences for repository utilization, based on simulation of an application of SKB's EFPC criteria along the tunnels. The results indicated that this type of fracture clustering did not have a significant effect on utilization factors for repository tunnels.

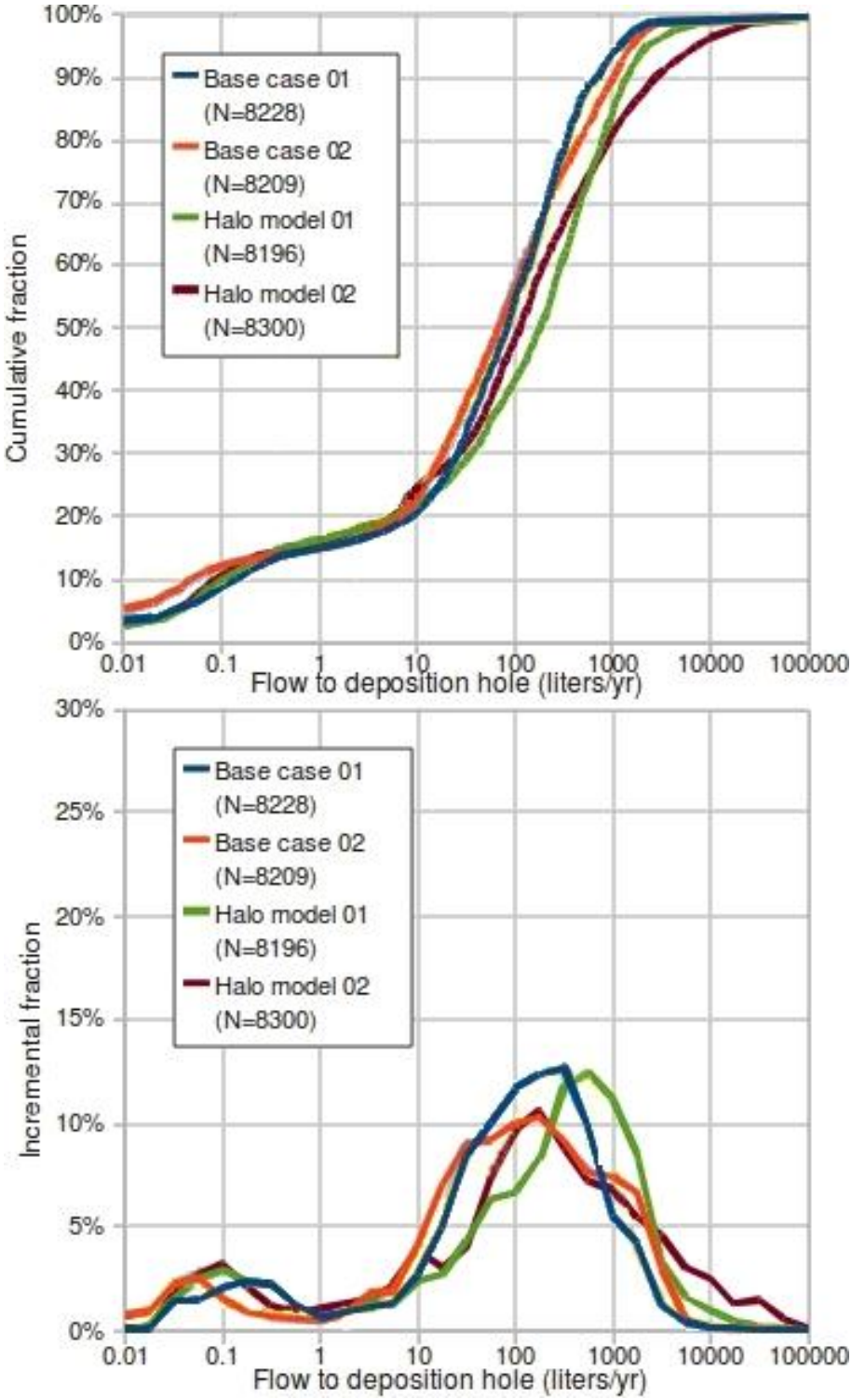

Figure 4.5: Distributions of flowrates to deposition holes from discrete-feature model simulations by Geier (2011c), comparing two realizations of the SR-Site base case Hydro-DFN model with two realizations of the halo model. Note that the curves (polylines) in the lower plot represent percentages for discrete increments of flowrate, rather than a continuous probability density function.

4.3.3. Variable-aperture/channelized DFN models

Variable-aperture models are a variation on ordinary DFN models, in which hydraulic properties of each fracture are considered to vary stochastically from point to point within the fracture plane. Tsang and Tsang (1989) showed that in a single fracture with flow aperture (related to transmissivity) that varies according to a geostatistical process, flow tends to coalesce into certain preferred flow paths, referred to as channels. This conceptualization of individual fractures was extended to a 3-D fracture network model by Nordqvist et al. (1996). Further review of the concept and comparison with experimental evidence of in-situ flow channelling was given by Tsang and Neretnieks (1998)

Much research on the effects of flow channelling due to aperture variation in fracture networks (including an evaluations by Painter, 2006 as part of SKB's research programme), has focused on the consequences for transport phenomena, particularly scale-dependent dispersion effects which result from transport in the resulting network of channels with mixing where channels meet, but otherwise independent transport along separate flow paths which may have different water velocities, retardation properties etc. However, a variable-aperture DFN model, if calibrated to the same type of borehole hydraulic-test data, could lead to different inferences regarding conductive fracture intensity and size distributions.

In the development of a hydrogeological DFN model for Olkiluoto, Hartley et al. (2012), while following an overall methodology similar to that applied in developing the Hydro-DFN model for Forsmark, considered a model variant in which only random patches occupying a fraction of the fracture surface area are open to flow, resulting in a degree of channelling. Patches are removed at random, so there is no systematic spatial correlation of transmissive vs. non-transmissive patches. Another difference with the variable-aperture models mentioned above is that all transmissive patches on a given fracture have a single value of transmissivity.

Hartley et al. (2012) calibrated this variant independently of two other variants which assumed uniform transmissivity throughout each fracture plane (i.e., the assumption embodied in all variants the SR-Site Hydro-DFN). The three calibrated model variants are then applied to model site-scale flow and transport, using CONNECTFLOW and a generally similar methodology to what has been presented for Forsmark.

The results in terms of flowrates to deposition holes (as presented in Figures 11-10 and 11-11 and discussed on p. 216 of Hartley et al., 2012) indicate that the distributions of flowrate, for the holes that are connected to the far-field network, are qualitatively similar for all three models, considering the stochastic variability between the limited number of realizations, and differences between the two models which assume uniform transmissivity in each fracture. However, the variant with discontinuous transmissivity results in slightly higher percentages of deposition holes being connected to the far-field network (25% to 31% depending on the repository panel for Model C, compared with 22% to 30% and 20% to 22% for the two uniformly-transmissive models, A & B).

This small influence (a few percent) on the number of flowing deposition holes should be seen as a lower bound on the sensitivity to aperture variation. More structured models of transmissivity variation (e.g. geostatistical models as considered by Tsang & Tsang, 1996) could lead to more spatially persistent channels in a given fracture. Correlation of transmissivity between adjoining fractures could have an even stronger effect on channel persistence. However, so far such models do

not seem to have been developed, calibrated and applied in situations that would allow a direct assessment of the impact on percentage of deposition holes that connect to a flowing network.

4.3.4. Sparse channel networks

Network models with more pronounced 3-D channelling effects can be produced either by considering lattices in which string- or pipe-like conductors are placed randomly between adjacent vertices of the lattice to yield a sparsely-connected pipe network, or from networks formed by random intersections of elongated, planar conductors in 3-D space – essentially a DFN model, but with transmissive features in the shape of elongated ellipses or rectangles, rather than circular or square fractures.

The properties of such models have been explored by Black et al. (2006 & 2007, plus recent publications in press) and have been discussed by Black (2011) in a previous review of SKB's hydrogeological models for Forsmark. The key property of a discrete-feature network model built out of elongated rather than equidimensional transmissive features is that the network begins to percolate at a lower intensity (total area of transmissive features per unit volume), and with a much lower density of junctions between conductive features. Sparse networks built up by the lattice approach were found to have similar properties.

As pointed out by Black (2011), a sparse channel network (conceptualized as a random system of elongated ellipse-shaped conductors) would yield a significantly more well-connected model that would percolate despite the apparent low intensity of conductive fractures.

In application to a forensic analysis of experiments carried out in the Stripa Mine in the 1980s, this type of model was successful in explaining the apparent positive "skin" effect that limited inflows to the tunnel, such that the inflows were significantly lower than were expected based on DFN models of the site. In the sparse channel network model, this effect arises from "hyper-convergent" flow due to the limited density of junctions in the water-conducting network. The model also leads to a compartmentalized flow system, in terms of hydraulic head and water chemistry.

Hyper-convergent flow effects in a sparse channel network could affect the interpretation of one of the main types of data that have been used to derive the Hydro-DFN: flowrates measured with the PFL during sustained pumping of a borehole. Flow convergence effects would tend to be less important (although not necessarily absent) in the other main situation in which the PFL has been used, open boreholes which are nominally at equilibrium. If the Hydro-DFN misrepresents the process of flow convergence to a pumped borehole, this would introduce errors into the results of the Hydro-DFN calibration which have not so far been addressed.

Hyper-convergent flow could also affect flowrates toward deposition holes and deposition tunnels during the resaturation period, gradually becoming less pronounced as the system reaches quasi-equilibrium and head gradients become more uniform. Convergence effects could persist in some cases if the tunnels themselves become dominant conductors in the post-closure flow system (e.g. due to the formation of a crown-space gap or a connected EDZ along the tunnels).

The consequences of a sparse channel network model for prediction of post-closure, post-saturation flows to deposition holes are difficult to assess either quantitatively or qualitatively. So far there does not seem to be an example of calibrating and applying a model based on this concept, for situations that are strongly analogous to the prediction of flowrates to deposition holes in a saturated system. Like the Hydro-DFN models that have been employed in SR-Site, a sparse-channel network model could have complex sensitivity to its controlling parameters that cannot necessarily be judged by intuition.

The abstract nature of the transmissive features in the models of Black et al. (2006 & 2007) – whether idealized as abstract "strings" on a lattice, or as elongated ellipses, randomly scattered in 3-D space – can be a barrier to intuitive understanding. From this point of view, it seems worthwhile to discuss how these features might relate to geologically observable features.

The concept of channelized flow in crystalline rock stems in part from direct observations showing that fractures tend to have variable aperture, in part from numerical modelling exercises such as the work of Tsang & Tsang (1989) which shows that this can lead to flow channelling, and generally small-scale experiments (either involving direct observation in laboratory replicas, or by interpretation of evidence from in-situ experiments). Some in-situ experiments seem to be very difficult to explain without channelling – notably a single-fracture experiment by Abelin et al. (1990) in which different tracers injected from two different points in a single fracture apparently crossed paths before reaching the points at which they were recovered (apparently due to channelling plus an intersecting fracture). From these various lines of evidence the concept is well-accepted, but there is still very poor understanding of what large-scale channels should "look like" in the rock.

Two different conceptual views can be considered:

- Channels arise from "dynamic" flow effects in variable-aperture fractures;
- Channels are fixed in position;

Models based on the concept of dynamic flow channelling in variable-aperture fractures have been discussed in the preceding section of this review. In such models, different channels may come into effect for flow in response to hydraulic gradients in different direction, so one would expect less extreme flow-convergence effects, and perhaps less of a distinction with uniform-aperture DFN models.

Models in which channels occupy a fixed position in space, regardless of the direction of head gradients, are represented by the lattice and ellipse-network models of Black et al. (2006 & 2007). These will be the focus of discussion in this section henceforth.

Fixed-position channels with elongated geometry could conceivably arise from geological processes including:

- Shear movements on a fracture with anisotropic roughness, resulting in elongated channels transverse to the direction of shear;
- Formation of gaps or breccia along the intersections between pairs of fractures, due to small shear movements;

- Precipitation/dissolution of fracture minerals that results in plugging of areas with small aperture that are not along a main path for fluid circulation;

- Alteration of fracture minerals in areas of small aperture, to produce clay minerals or other alteration products that can clog these areas.

Among these processes, precipitation/dissolution and alteration processes have the potential to form channels that persist from one fracture to the next, rather than being restricted to a single fracture plane or the intersection between a pair of planes. Networks formed by such persistent channels, produced by gradually pinching off of a prior flow field by mineral precipitation or alteration, could conceivably percolate at even lower spatial densities than sparse channel network models that are simulated by stochastic geometrical models (such as random ellipses).

A sparse-channel network model could be calibrated to site data without considering the geological origins of the channels, simply by adjusting parameters in a manner analogous to what SKB has done in fitting their Hydro-DFN model by adjusting the parameters of the fracture size distribution and the transmissivity-size relationship. Without going through this exercise, the outcome is very difficult to predict – even whether it will yield a single best-fit parameterization, or a suite of equally probable parameterizations.

An alternative approach could be to begin with an assumption about how the channels are related to the fractures which are observable at the surface of the site, and also in boreholes, and eventually (if approved for construction) in tunnels underground.

For example, one could begin with the assumption that all fractures in the Geo-DFN model contain channel-like conductors, which are randomly oriented on each given fracture, and a further assumption that channels on one fracture are not genetically related to channels on any another fracture.

A numerical model based on these two assumptions has been partly developed for exploratory calculations as part of this review, but thus far usable results have not been obtained. Further exploratory calculations are planned in connection with the ongoing evaluation of the Geo-DFN model as mentioned above.

5. The Consultant's overall assessment

SKB's conceptual model for flow through the fractured bedrock at repository depth is based on a binary division into hydraulic conductor domains (HCDs) versus the remainder of the rock, the hydraulic rock domain (HRD). The HRD in turn is subdivided into different fracture domains and depth intervals, with different statistical Hydro-DFN models depending on the fracture domain and depth. This review has focused mainly on the description of the fracture domains FFM01 and FFM06 for depths below z = -400 m, which effectively serve as the host rock for the deposition areas in the proposed repository.

Assessment of HCD component of model

The HCD portion of the model is relatively well-characterized by the field investigations and site-descriptive modelling, but it relies on several assumptions that are not well supported by the data and have not been addressed by alternative models or parameterizations:

- Steeply dipping HCDs are subject to the same decrease in hydraulic conductivity with depth as has been assessed for the more well-characterized, gently dipping zones.
- HCDs have locally isotropic conductivity.
- When represented as heterogeneous, HCDs have very limited correlation of properties in the vertical direction.

These assumptions, if incorrect, may lead to moderate underestimation of groundwater flux through the repository volume, by limiting the possibility for vertically oriented bands of high hydraulic conductivity in the HCDs to continue to repository depths. However, considering that the influence of these HCDs is limited by the relatively tight HRD, the impact of these assumptions on near-field flows is likely small in relation to uncertainties in HRD properties.

Assessment of HRD component of model for host rock

The greatest cause for concern with the HRD is that very few alternative concepts or parameterizations have been considered, particularly for the host rock around the proposed deposition panels. This host rock is the geosphere component that most directly controls flowrates to deposition holes, but the Hydro-DFN is poorly constrained by data and calibrations.

The Hydro-DFN model for Fracture Domain FFM01 (also used for FFM06) below a depth of 400 m makes very limited use of geometrical information from the Geo-DFN. Parameter estimates were developed mainly by a combination of forward-modeling and trial-and-error adjustments, to improve the resemblance of model predictions to measurements (mainly flowing fracture frequencies and specific capacities from differential flowmeter logging in deep core-drilled holes). The

fracture size distribution and three hypothesized transmissivity-size relationships were both calibrated by this approach.

The match of simulated data to measured data, at the end of this trial-and-error process, is not especially convincing, especially when one considers that a large fraction of the fractures in the Hydro-DFN model are assessed as having transmissivities below the measurement threshold of the hydraulic testing equipment. The limited set of Hydro-DFN model variants that have been evaluated are not sufficient to provide a systematic assessment of the model's sensitivity, either to the adjustable parameters or to the resolution of the hydraulic measurements. The significance of variation between stochastic realizations of the Hydro-DFN model was also not systematically evaluated.

No alternative hydrogeological conceptualizations of the repository host rock are presented that are independent of the Hydro-DFN model. The only models mentioned as alternatives (CHAN3D and ECPM/CPM models) use parameters that are partly or entirely derived from the Hydro-DFN.

Only a few alternative parameterizations were propagated to the point of calculating near-field fluxes. Among the list of hydrogeological variants considered for temperate climates, the only variants that really concern the Hydro-DFN for the host rock are the two transmissivity-size models ("correlated" and "uncorrelated") that were considered as alternatives to the central ("semi-correlated") case.

Assessment of alternative models for the host rock

This review has considered four types of alternative models for the HRD that have not been considered in SKB's analysis.

Two of these are DFN models that include heterogeneity in terms of fracture intensity:

- Fracture intensity varying according to a gamma distribution as suggested by SKB's Geo-DFN analysis;
- Fracture intensity correlated to minor deformation zones according to a "halo" model.

Possible consequences of these alternative models include a moderate (possibly twofold) increase in the number of deposition holes with relatively high flows, and up to an order of magnitude increase in the maximum flowrates to be considered. The heterogeneous-intensity models could also produce a clustering of deposition holes that are subject to high flowrates, within a given realization of the repository.

The other two types of models discussed here involve some degree of channelling:

- Variable-aperture DFN models; and
- Sparse channel network models.

A limited assessment has been made of a very simplified version of a variable-aperture DFN model, in support of Finland's repository programme. The model assumes that any given fracture is non-transmissive on randomly distributed patches

occupying some specified fraction of its area, with no larger-scale correlations. The main effect observed for the model of the Olkiluoto site in Finland was an increase of a few percent in the number of deposition holes that are connected to the flowing fracture network. A more pronounced effect could be expected from a more realistic aperture-variation model that produces more extensive, coherent channels across fractures.

Sparse-channel network models have not thus far been applied in situations directly analogous to simulation of flows to deposition holes in a repository. Research applications to simulate flow to open tunnels showed that this type of model can explain the so-called “tunnel skin” effects which have been inferred from studies in underground laboratories in sparsely fractured crystalline rock, due to the effects of flow convergence in a sparsely connected network. Convergent flow phenomena in such a conceptual model could also be expected to influence flow-meter measurements under pumped-borehole conditions – that is, the primary data used for estimating parameters of the Hydro-DFN model.

The current level of development of most of the alternative models considered here is not sufficient to provide firm, quantitative estimates of the impacts of these alternatives on the flowrate distributions. Further investigation of strongly channelled models is recommended to provide better bounds on the possible effects.

6. References

Abelin, H., Birgersson, L., Widén, H. and Ågren, T., 1990. Channelling experiment. Stripa Project Technical Report 90-13, SKB.

Black, J., 2012. Selective review of the hydrogeological aspects of SR-Site. SSM Technical Note 2012:37, SSM.

Black, J.H., Robinson, P.C., and Barker, J.A., 2006. A preliminary investigation of the concept of 'hyper-convergence' using 'sparse' channel networks. Report R-06-30, SKB.

Black, J.H., Barker, J.A., and Woodman, N.D., 2007. An investigation of 'sparse channel networks' Characteristic behaviours and their causes. Report R-07-35, SKB.

Crawford, J., 2008. Bedrock transport properties Forsmark. Site descriptive modelling SDM-Site Forsmark. Report R-08-48, SKB.

Darcel, C., Davy, P., Bour, O., De Dreuzy, J-R, 2006. Discrete fracture network for the Forsmark site. Report R-06-79, SKB.

Follin, S., 2008. Bedrock hydrogeology Forsmark. Site descriptive modelling, SDM-Site Forsmark. Report R-08-95, SKB.

Follin, S., Stigsson, M., and Svensson, U., 2005. Regional hydrogeological simulations for Forsmark – numerical modelling using DarcyTools. Preliminary site description Forsmark area – version 1.2. Report R-05-60, SKB.

Follin, S., Hartley, L., Jackson, P., Roberts, D., and Marsic, N., 2008. Hydrogeological conceptual model development and numerical modelling using CONNECTFLOW. Forsmark modelling stage 2.3. Report R-08-23, SKB.

Follin, S., Levén, J., Hartley, L., Jackson, P., Joyce, S., Roberts, D., and Swift, B., 2007a. Hydrogeological characterisation and modelling of deformation zones and fracture domains. Forsmark modelling stage 2.2. Report R-07-48, SKB.

Follin, S., Johansson, P-O., Hartley, L., Jackson, P., Roberts, D., and Marsic, N., 2007b. Hydrogeological conceptual model development and numerical modelling using CONNECTFLOW, Forsmark modelling stage 2.2. Report R-07-49, SKB.

Fox, A., La Pointe, P., Hermanson, J., and Öhman, J., 2007. Statistical geological discrete fracture network model for the Forsmark site. Site descriptive modelling Forsmark stage 2.2. R-07-46, SKB.

Fox, A., Forchhammer, K., Pettersson, A., La Pointe, P., and Lim, D-H., 2012. Geological discrete fracture network model for the Olkiluoto site, Version 2. Posiva 2012-27. Posiva Oy.

Frampton, A., 2010. Stochastic analysis of fluid flow and tracer pathways in crystalline fracture networks. PhD Thesis, Royal Technical Institute, Stockholm, Sweden.

Geier, J., 2011a. Hydrogeological conditions at the Forsmark site. Technical Note 2012:41, SSM.

Geier, J., 2011b. Hydrogeological modelling of the Forsmark site. Technical Note 2012:67, SSM.

Geier, J., 2011c. Investigation of discrete-fracture network conceptual model uncertainty at Forsmark. SSM Research Report 2011:13, SSM.

Hartley, L., Appleyard P., Baxter, S., Hoek, J., Roberts, D., and Swan, D. 2012. Development of a Hydrogeological Discrete Fracture Network Model of Olkiluoto; Site Descriptive Model 2011. Working Report 2012-32. Posiva.

Hartley, L., and Joyce, S., Responses to SSM on Hydrogeology. SKBdoc id 1396325, 23rd May 2013, SKB.

INSITE, 2007. Consolidated Review Issues: The CRI List. INSITE M-08-xx, SSM.

Joyce, S., Simpson, T., Hartley, L., Applegate, D., Hoek, J., Jackson, P., Swan, D., Marsic, N., and Follin, S., 2009. Groundwater flow modelling of periods with temperate climate conditions – Forsmark. Report 2009-20, SKB.

Laaksoharju, M., Smellie, J., Tullborg, E-L., Gimeno, M., Hallbeck, L., Molinero, J., and Waber, N., 2008. Bedrock hydrogeochemistry Forsmark. Site descriptive modelling, SDM-Site Forsmark. Report R-08-47, SKB.

La Pointe, P. R., Olofsson, I., and Hermanson, J., 2005. Statistical model of fractures and deformation zones for Forsmark: Preliminary site description Forsmark area – version 1.2. Report R-05-26, SKB.

Liu, L., Moreno, L., Neretnieks, I., and Gylling, B., 2010. A safety assessment approach using coupled NEAR3D and CHAN3D – Forsmark. Report R-10-69, SKB.

Munier, R., 2010. Full perimeter intersection criteria. Definitions and implementations in SR-Site. SKB TR-10-21, SKB.

Nordqvist, A.W., Tsang, Y.W., Tsang, C-F., Dverstorp, B., and Andersson, J., 1992. A variable aperture fracture network model for flow and transport in fractured rocks. *Water Resources Research*, Vol. 28, No. 6, p. 1703–1713.

Olofsson, I., Simeonov, A., Stephens, M., Follin, S., Nilsson, A-C., Röshoff, K., Lindberg, U., Lanaro, F., Fredriksson, A., and Persson, L., 2007. Site descriptive modelling Forsmark, stage 2.2: Presentation of a fracture domain concept as a basis for the statistical modelling of fractures and minor deformation zones, and interdisciplinary coordination. Report R-07-15, SKB.

Painter, S., 2006. Effect of single-fracture aperture variability on field-scale transport. Report R-06-25, SKB.

Posiva, 2012. Olkiluoto Site Description 2011. Posiva 2011-02, Posiva Oy.

Robinson, P.C., 1984. Connectivity of fracture systems – A percolation theory approach, *J. Phys. A, Math. Gen.*, 16, 605-614.

Selroos, J-O., and Follin, S., 2010. SR-Site groundwater flow modelling methodology, setup and results. Report R-09-22, SKB.

SKB, 2008. SDM-Site site description of Forsmark at completion of the site investigation phase, SDM-Site Forsmark. SKB R-08-05, SKB.

Stephens, M. B., Fox, A., La Pointe, P., Simeonov, A., Isaksson, H., Hermanson, J., and Öhman, J., 2007. Geology Forsmark. Site descriptive modelling Forsmark stage 2.2. Report R-07-45, SKB.

Svensson, U., and Follin, S., 2009. Groundwater flow modelling of the excavation and operational phases – Forsmark. Report R-09-19, SKB.

Terzaghi, R., 1965. Sources of error in joint surveys. *Geotechnique* Vol. 15, No. 3, p. 287–304.

Tsang, C-F, and Neretnieks, I, 1998. Flow channelling in heterogeneous fractured rocks. *Reviews of Geophysics*, Vol. 36, No. 2, p. 275–298.

Y. W. Tsang, Y.W., and Tsang, C.F., 1989. Flow channeling in a single fracture as a two-dimensional strongly heterogeneous permeable medium. *Water Resources Research*, Vol. 25, No. 9, p. 2076–2080. DOI: 10.1029/WR025i009p02076

Tsang, Y.W., Tsang, C. F., Hale, F.V., and Dverstorp, B., 1996. Tracer transport in a stochastic continuum model of fractured media. *Water Resources Research*, Vol. 32, No. 10, p. 3077, doi:10.1029/96WR01397.

Vidstrand, P., Follin, S., and Zugec, N., 2010. Groundwater flow modelling of periods with periglacial and glacial climate conditions – SR-Site Forsmark. Report R- 09-21, SKB.

Öhman, J., and Follin, S., 2010. Hydrogeological modelling of SFR. Data review and parameterisation of model version 0.1. Site investigation SFR. Report P-09-49, SKB.

APPENDIX 1

Coverage of SKB reports

Table A1:1

Reviewed report	Reviewed sections	Comments
SKB R-07-46, Statistical geological discrete fracture network model for the Forsmark site. Site descriptive modelling Forsmark stage 2.2.	Mainly Sections 5 & 7 (uncertainty analysis and model summary)	Reviewed from perspective of whether key conclusions and uncertainties were transferred to the HydroDFN analysis.
SKB R-07-48 Hydrogeological characterisation and modelling of deformation zones and fracture domains. Forsmark modelling stage 2.2.	All	Key report describing HCD description and Hydro-DFN model derivation and calibration.
SKB R-07-49, Hydrogeological conceptual model development and numerical modelling using CONNECTFLOW, Forsmark modelling stage 2.2.	All	Key report describing Hydro-DFN model calibration and comparison of integrated model to field data.
Report R-08-23, Hydrogeological conceptual model development and numerical modelling using CONNECTFLOW. Forsmark modelling stage 2.3	All	Largely recapitulates R-07-48 and R-07-49.
SKB R-08-95, Bedrock hydrogeology Forsmark. Site descriptive modelling, SDM-Site Forsmark.	All	Overview report.
SKB R-09-19 Groundwater flow modelling of the excavation and operational phases – SR Site Forsmark	Mainly Sections 3 & 4 considered for this review.	Focus on how Hydro-DFN model was implemented.
SKB R-09-20 Groundwater flow modelling of periods with temperate climate conditions – Forsmark	All	Primary focus in terms of consequences of Hydro-DFN for safety assessment.
SKB R-09-21 Groundwater flow modelling of periods with periglacial and glacial climate	Mainly Sections 3 & 4 considered for this review.	Focus on how Hydro-DFN model was implemented.

conditions		
SKB R-09-22 SR-Site groundwater flow modelling methodology, setup and results	All	Good overview report of hydrogeological modelling.
SKB TR-10-21 Full perimeter intersection criteria. Definitions and implementations in SR-Site, Updated 2013-02	Main findings and conclusions only	Minor focus as background for this review.
SKB TR-10-52 Data report for the safety assessment SR-Site	Sections 6.3 & 6.6	Considered how site-descriptive model transferred over into data definitions for SR-Site.
Complementary information to SKB's application requested by SSM.	Both memoranda (SKB and Hartley & Joyce); data deliveries examined but not reviewed in detail.	Main topic of concern for this review is to be addressed by an SKB delivery in December 2013.

2014:05

The Swedish Radiation Safety Authority has a comprehensive responsibility to ensure that society is safe from the effects of radiation. The Authority works to achieve radiation safety in a number of areas: nuclear power, medical care as well as commercial products and services. The Authority also works to achieve protection from natural radiation and to increase the level of radiation safety internationally.

The Swedish Radiation Safety Authority works proactively and preventively to protect people and the environment from the harmful effects of radiation, now and in the future. The Authority issues regulations and supervises compliance, while also supporting research, providing training and information, and issuing advice. Often, activities involving radiation require licences issued by the Authority. The Swedish Radiation Safety Authority maintains emergency preparedness around the clock with the aim of limiting the aftermath of radiation accidents and the unintentional spreading of radioactive substances. The Authority participates in international co-operation in order to promote radiation safety and finances projects aiming to raise the level of radiation safety in certain Eastern European countries.

The Authority reports to the Ministry of the Environment and has around 270 employees with competencies in the fields of engineering, natural and behavioural sciences, law, economics and communications. We have received quality, environmental and working environment certification.

Strålsäkerhetsmyndigheten
Swedish Radiation Safety Authority

SE-171 16 Stockholm
Solna strandväg 96

Tel: +46 8 799 40 00
Fax: +46 8 799 40 10

E-mail: registrator@ssm.se
Web: stralsakerhetsmyndigheten.se